Final Draft
of the original manuscript:

Halder, K.; Khan, M.M.; Gruenauer, J.; Shishatskiy, S.; Abetz, C.;
Filiz, V.; Abetz, V.:

Blend membranes of ionic liquid and polymers of intrinsic microporosity with improved gas separation characteristics

In: Journal of Membrane Science (2017) Elsevier

DOI: 10.1016/j.memsci.2017.06.022

Blend Membranes of Ionic Liquid and Polymers of Intrinsic Microporosity with Improved Gas Separation Characteristics

Karabi Halder[1], Muntazim Munir Khan[1], Judith Grünauer[1], Sergey Shishatskiy[1], Clarissa Abetz[1], Volkan Filiz[1], Volker Abetz[1,2]

[1] *Helmholtz-Zentrum Geesthacht, Institute of Polymer Research, Max-Planck-Strasse 1, 21502 Geesthacht, Germany*

[2] *University of Hamburg, Institute of Physical Chemistry, Martin-Luther-King-Platz 6, 20146 Hamburg, Germany*

Corresponding author: volkan.filiz@hzg.de (V. Filiz)

Tel No.: +494152 87 2425; fax: +494152 87 2499

Abstract:

In the present work an attempt has been made for the first time to blend polymers of intrinsic microporosity, specifically PIM-1 with the ionic liquid (IL) [C_6mim][Tf_2N] in order to improve the gas separation properties of PIM membranes. The blend membrane led to a slightly reduced permeability and improved the selectivity. However, due to the lack of compatibility between PIM-1 and the IL, the polarity of PIM-1 had to be tuned. Blending and chemical modifications of PIM-1 were studied to achieve a good distribution of the IL in the polymer matrix. The first method included physical blending of PIM-1 with poly(ethylene glycol) (PEG) as compatibilizer and the second method included copolymerization of PIM-1 monomers with a PEG containing anthracene maleimide comonomer (CO). The copolymerization technique yielded better polymer-IL compatibility in the IL concentration range 2.5 – 10 wt.% compared to the blends of PIM-1 with PEG and IL. The incorporation of the IL into the copolymer of PIM-1 (PIM-COP) matrix resulted in an improvement of CO_2/N_2 selectivity from 19 to 30 at 30°C, in combination with a relatively high CO_2 permeability coefficient (above 800 Barrer). The studied polymer-IL composites are good candidates for the use as selective layer materials in thin film composite membranes aimed at e.g. post-combustion gas separation.

Keywords: Polymers of Intrinsic Microporosity (PIMs)
Ionic Liquids (ILs), PIM-1 copolymer
Membranes, Gas Separation

1. Introduction

Gas separation plays a pivotal role in the chemical industry owing to its array of applications ranging from carbon dioxide removal, hydrogen recovery to sequestration of valuable components from waste gas streams [1]. Compared to the other conventional gas separation approaches such as pressure swing adsorption or cryogenic distillation, membrane technology is the most pragmatic solution due to its low energy consumption, small footprint and ease of operation [2, 3].

The corner stone of the membrane separation process is the material of the selective layer. Polymeric membranes have proved to be reliable in numerous applications for separation of various gas mixtures. But the need for new membranes working at harsh conditions or having higher permeance and selectivity and thus lower operational and investment costs of separation units, boosts the research in the field of polymers and polymer based materials for gas separation membranes. Despite the rapid progress in the development of new polymers, the trade-off between permeability and selectivity as demonstrated by Robeson [4] is hardly overcome. The need for improvement in gas transport properties of polymeric materials to make them suitable for membrane gas separation applications has made the understanding of relation of polymeric structure and gas transport properties quite demanding [5, 6]. One of the promising ways of obtaining polymer based composite materials with gas transport properties beyond the Robeson's upper bound is to combine polymers with other attractive solid or liquid compounds . The unique and synergetic properties of the fillers when dispersed in the polymer matrix provide desired shift of properties. Numerous glassy polymers possessing high fractional free volume (FFV) have been discovered in the recent past, such as thermally rearranged polymers, covalent organic frameworks, conjugated microporous polymers, substituted polyacetylenes, perfluoro-polymers and polymers of intrinsic microporosity (PIMs)[7-11] and can be used in combination with the specific filler materials to form composite material with outstanding properties.

The microporous, glassy, high free volume polymers, that have received abundant attention in the recent past, are the polymers of intrinsic microporosity (PIMs), first reported by Budd and McKeown [12, 13]. Among the PIMs synthesized, PIM-1 is by far the most widely investigated polymer, firstly because of its relative ease of synthesis, and secondly due to its promising gas permeation properties. As described in earlier publications [12, 14], the

sites of contortion embedded in the PIM-1 backbone force the formation of large and well interconnected free volume elements, making the polymer highly permeable but moderately selective for technically important gas pairs e.g. CO_2/N_2 and CO_2/CH_4. However, an improvement in the separation selectivity even when it will be accompanied with some losses in permeability, is desirable in order to promote the use of this material as a membrane selective layer.

The intrinsic microporosity of PIMs has been studied to find the way to ameliorate the gas transport properties of these polymers. The vast majority of monomers or comonomers with rigid structural components having well-defined concavities [15] enable tailoring of the gas transport properties of PIMs and give one the possibility to molecularly design the new membrane material with improved selectivity and stability over time [16]. A better interaction of the polymer with the incoming penetrant had been realized by the post-synthetic modification of the cyano- group in PIM-1 to carboxylate, thioamide and tetrazole groups[17-19] and copolymerization to phenylsulfone and trifluoromethyl groups [20]. The PIMs copolymerized with anthracene based comonomers exhibited lower permeability with only moderate increase or comparable selectivity which could be tuned by careful adjustment of the interchain packing and enhancement of the polymer backbone rigidity [21]. Thermal treatment of the carboxylated PIMs [22], UV-photochemical treatment of polymers containing dispersed ZIF-71 nanoparticles [2] and chemical crosslinking with PEG-biazide via nitrene reaction [3] are techniques successfully implemented on PIMs. These techniques lead to stabilization of the polymeric membranes and are manifested with an increase in gas pair selectivity e.g. CO_2/N_2 selectivity.

Amongst the aforementioned techniques for improving the gas transport properties of PIMs, the physical blending approach has been recognized as one of the cost effective and fast alternatives to obtain an improvement in physical properties of the pristine PIM-1 polymer [23]. This versatile tool synergistically combines the beneficial properties of two or more compounds in one single material which is difficult to obtain by other means. Although a very competitive approach, some major drawbacks of physical blending cannot be ruled out [23]. The miscibility of the blend components and homogeneity of the resulting material are two of its primary limitations. The blend can be categorized in principle into the following three types: miscible, immiscible and partly miscible. The miscible blends are single phase systems where the components homogenize with each other at a molecular level and often show physical properties in between those of individual components. On the contrary, in an immiscible blend, components are found in separate phases and don't show shift of e.g. glass

transition temperatures towards each of the component's values [24]. Partially miscible blends also known as isotropic heterogeneous blends [25] have properties in between the miscible and immiscible blends.

Until now, work has been done incorporating poly(ethylene) glycol (PEG) [26] and Matrimid® 5218 [23] in different concentrations to PIM-1 for adjusting the microstructure, and hence the diffusion, solubility and selectivity of the glassy polymer. In either of the blends, properties of components allowed for synergistic improvement of the resulting material properties giving mechanically robust and superior gas separation performance membranes.

In addition to the blending of PIM-1 with polymers or other solid fillers, liquids and particularly ionic liquids (ILs) can offer attractive transport features when combined with the polymer due to their low resistance to penetrant's diffusion [27]. Along with their high gas diffusivity ILs can gain excellent selectivity for a desired gas pair by tuning the composition of functional groups. The inability to form a stable crystal lattice due to the poorly coordinated ion in ILs, causes these unique materials to remain as a liquid at or near room temperature. Widely promoted as green solvents, the ILs have received significant attention due to their chemical and thermal stability, negligible vapor pressure and high solubility for organic and inorganic species [28]. The low melting point and stability under a wide range of processing conditions enable the room temperature ionic liquids (RTILs) with imidazolium or pyridinium cations to be most commonly used. Chen et al. demonstrated for the first time a polymer blend comprising of poly(vinylidene fluoride) (PVDF) and the RTIL 1-ethyl-3-methylimidazolium tetracyanoborate ([emim][$B(CN)_4$]) showing high CO_2 permeability and CO_2/N_2 selectivity of 1778 Barrer and 41 respectively [29]. The enhanced solubility of CO_2 in ILs yielded the high selectivity while PVDF provided the mechanical strength to the membrane. In another study Liang et al. have exploited the beneficial properties of [C_4mim][Tf_2N] and PMDA-ODA-PA as a composite blend for superior gas separation performance [30]. Based on these investigations, it is expected that the highly permeable PIM-1 will be reduced in permeability but would gain some selectivity by blending with the IL.

Owing to the hydrophobicity of the PIM-1 polymer, the relatively hydrophobic IL 1-hexyl-3-methyl imidazolium bis(trifluromethyl sulphonyl) imide [C_6mim][Tf_2N] (structure shown in Fig.1) has been chosen in the current study as the filler for the polymer matrix. Apart from the thermal and chemical stability of the IL the capacity of the liquid filler to dissolve CO_2, CH_4, C_2H_6, C_2H_4 makes it particularly interesting for a variety of applications

such as solvent in reactions, as gas storage media and in CO_2/N_2 separation [31, 32]. Although the cation 1-hexyl-3-methyl [C_6mim], plays a secondary role in controlling the gas transport selectivity, the relatively long hexyl chain renders the maximum hydrophobic character to the ionic liquid as compared to its ethyl and butyl counterparts, thus making it a promising candidate for blending with the hydrophobic PIM-1. At the same time the CO_2 permeability of the IL and PIMs are much closer to each other than for polymers as described above. The CO_2 permebility coefficient of [C_6mim][Tf_2N] is also higher than most of the of polymers studied so far.

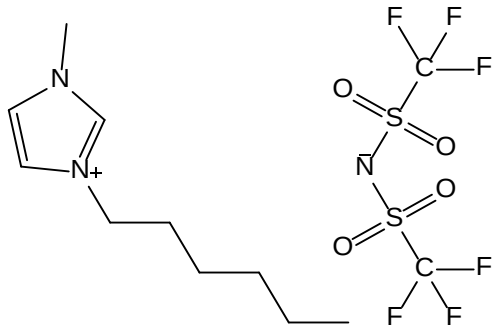

Figure 1**.** Chemical structure of [1-hexyl-3-methyl imidazolium bis(trifluromethyl sulphonyl) imide [C_6mim][Tf_2N]

The aim of this work is to prepare blend membranes of [1-hexyl-3-methyl imidazolium bis(trifluromethyl sulphonyl) imide [C_6mim][Tf_2N] IL and PIM-1 to take advantage of the high permeability of PIM-1 and relatively high permeability of the [C_6mim][Tf_2N] and to investigate the influence of the IL on the gas selectivity (e.g. CO_2/N_2) of the blend . To further enhance the compatibility of PIM-1 with [C_6mim][Tf_2N], a modification to the PIM-1 has been made by two techniques. The first included physical blending of PEG and PIM-1 for better IL distribution and the second involved copolymerization with a PEG containing anthracene maleimide monomer to enhance its hydrophilicity. The compatibility of components or the blend homogeneity and morphology of the prepared blends were studied using contact angle tests and scanning electron microscopy (SEM). The single gas permeation properties, the permselectivity and the sorption measurements of the copolymer blends have been studied for an understanding of O_2, N_2, CO_2 and CH_4 gas transport characteristics.

2. Experimental

2.1. Materials

5,5´,6,6´-tetrahydroxy-3,3,3´,3´-tetramethyl-1,1´-spirobisindane (**TTSBI)** (97%) was purchased from ABCR GmbH and Co. KG (Karlsruhe, Germany); 2,3,5,6-tetrafluoroterephthalodinitrile (**TFTPN**) was donated by Lanxess (Bitterfeld, Germany) and was sublimated twice at 70°C under a pressure of 10^{-3} mbar before use. PEO 44 maleimide was obtained from Specific Polymers (France). Potassium carbonate (K_2CO_3, > 99.5%) was dried overnight under vacuum at 120°C and milled in a vibratory mill for 10 min. Dimethyl acetamide (DMAc, ≥ 99%), dimethyl formamide (DMF, ≥ 99%), boron tribromide (BBr_3), tetrahydrofuran (THF, ≥ 99.9%), methanol (CH_3OH, ≥ 99.9%), chloroform ($CHCl_3$, 99.9%), and ILs 1-ethyl-3-methyl imidazolium bis (trifluoromethylsulphonyl) imide [C_2mim][Tf_2N], 1-butyl-3-methyl imidazolium bis (trifluoromethylsulphonyl) imide [C_4mim][Tf_2N], and 1-hexyl-3-methyl imidazolium bis (trifluoromethylsulphonyl) imide [C_6mim][Tf_2N] were obtained from Merck and were used without further treatment. An anodized alumina membrane Anodisc® with support ring of 47 mm diameter and 0.02 µm pore size, thickness of 50 microns was purchased from GE Healthcare GmbH. The other commercially available reagents were obtained from Sigma-Aldrich (Germany) and were used without further treatment.

2.2. Monomer synthesis

2.2.1 2,3,6,7-Tetramethoxy-9,10-dibutylanthracene

Pentanal (23 g, 0.27 mol) was added dropwise at 0–5 °C to a stirred cooled mixture of (1,2-dimethoxybenzene) (21.6 g, 0.16 mol) in concentrated H_2SO_4 (70% - 50 ml) over a period of 1 h. The reaction mixture was stirred at room temperature for 3 days and poured into a 1 litre solution containing ethanol:water (1:1). The precipitate was filtered, washed with 250 ml acetone and dried to give a yellow powder (10g, 30%), m.p: 218–220 °C. ^{1}H-NMR (500 MHz, $CDCl_3$): δ (ppm): 1.06 (t, 6H), 1.61 (m, 4H), 1.81 (m, 4H), 3.42 (t, 4H), 4.06 (s, 12H), 6.84 (s, 2H), 6.87 (s, 2H). FT-IR: 3006, 2949, 2960, 2828, 1633, 1553, 1434, 1239, 1199, 1189, 1164, 1013, 892, 828, 750 cm^{-1}.

2.2.2 2,3,6,7-Tetrahydroxy-9,10-dibutylanthracene

2,3,6,7-Tetramethoxy-9,10-dibutylanthracene (4.5 g, 10.96 mmol) was dissolved in 70 ml dichloromethane (DCM) and added slowly with cooling in an ice-bath to boron tribromide (1.6 ml, 16.8 mmol), dissolved in 40 ml DCM under argon atmosphere. The reaction mixture was stirred at room temperature for 18 h, and then 20 ml of water was added slowly to destroy the excess boron tribromide. The contents were precipitated in water (1 litre) and stirred for 2

days for complete precipitation. The precipitate was filtered and washed with copious amounts of water, dried in vacuum at 60 °C to give a grey solid (2.5 g, 85%), mp: 210°C, ^{1}H-NMR (300 MHz, DMSO-d6) δ: 1.02 (t, 6H), 1.57 (m, 8H), 3.19 (t, 4H), 7,33 (s, 4H), 9.39 (br, 4H), FT-IR: 3378, 2954, 2924, 1650, 1501, 1447, 1383, 1319, 1292, 1251, 1209,1148,1093, 997, 844, 754.cm^{-1}.

2.2.3 2,3,6,7-Tetrahydroxy-9,10 dibutyl-13-poly (oxyethylene)-9,10-dihydro-9,10 [3,4]epipyrroloanthracene -12,14-dione (CO)

A mixture of 2,3,6,7-tetrahydroxy-9,10-dibutylanthracene (0.5 g, 1.41 mmol) and PEO-44 maleimide (3.25 g, 1.55 mmol) in p-xylene (100 ml) was refluxed for 24 h. The solvent was removed from the grey suspension using short way distillation under reduced pressure to give a dark brown solid (3.12 g, 86%), mp: 46°C, **1**H NMR (300MHz, DMSO-d6) δ: 1.07 (t, 6H), 1.66(m, 4H), 1.91(m, 2H), 2.08(m, 2H), 2.64(m, 2H), 2.73(s, 2H), 3.13(s, 2H), 3.5(s, PEG, 176H), 6.65(s, 2H), 6.73(s, 2H), 8.67(s, 2H), 8.72(s, 2H). ^{13}C NMR (90 MHz, DMSO-d6) δ: 15.5, 23.5, 27.0, 36.9, 45.3, 58.4, 66.3, 70.1, 71.6, 110.3/111.3, 134.4/136.2, 142.4/142.8, 176.1, FT-IR: 2880, 1766, 1466, 1359, 1280, 1239, 1101(s), 1059, 595, 841 cm^{-1}, Elemental analysis: calculated: C = 57.3 %, H = 8.59%, N = 0.59%, found: C = 56.99%, H= 8.70%, N = 0.67%, $TGA_{(onset)}$: 310°C.

2.3. Polymer synthesis

2.3.1 Synthesis of PIM-1

A fast synthesis method was employed for the synthesis of high molecular weight PIM-1, originally introduced by Guiver et al. [32]. A slight modification of the approach was made as follows: in a three necked round-bottomed flask fitted with a condenser, TTSBI and TFTPN were dissolved in DMAc in equimolar amounts to form an orange-red solution under argon atmosphere. Addition of excess K_2CO_3 (2.3 times with respect to the -OH monomer concentration) caused a color change to yellow. Transfer to an oil bath (150°C) caused the formation of a foamy suspension, accompanied by an increase in the viscosity of the solution. Gradual addition of diethylbenzene (DEB) (approximately the same amount as DMAc) lowered the viscosity enabling smooth stirring. The suspension was stirred for another 0.5 hour, precipitated in methanol and filtered off. Boiling the isolated polymer in water for one hour resulted in the removal of the residual solvents and salts. The polymer was collected by filtration and dried at 70°C under vacuum. The final purification step comprised of dissolving

the dried polymer in minimal $CHCl_3$ and re-precipitating in excess CH_3OH. Suction filtration followed by drying in vacuum overnight at 60°C yielded the yellow PIM-1 polymer (90% yield). The apparent molecular weight (Mw) and polydispersity index (PDI) were determined by gel permeation chromatography as 1.50 x 10^5 g mol^{-1} and 4.6, respectively.

2.3.2 Synthesis of copolymer (PIM1_CO_2.5) (PIM-COP)

This copolymer synthesis was inspired from the low temperature approach of polycondensation of PIM-1 originally proposed by Budd et al. [12]. In a three-necked round bottomed flask equipped with condenser and argon inlet, the monomer TTSBI and comonomer (**CO**) mixed in the ratio (97.5 : 2.5) along with TFTPN were stirred in dry DMF until complete dissolution. Addition of excess K_2CO_3 (2.3times) to the transparent mixture changed the color from brown to yellow. The contents were transferred to an oil bath maintained at 55°C and left stirring for 15 days. Progress of polycondensation was followed by sampling. After cooling, the contents were precipitated in water and dried in a vacuum oven overnight at 90°C. Repeated dissolution in $CHCl_3$ and re-precipitation in CH_3OH yielded the chrome yellow polymer (90% yield). The average molecular weight of the synthesized polymer was found to be 1.23 x 10^5 (g mol^{-1}) and the PDI of the prepared copolymer was found to be 4.6.

2.4. Blend preparation

In order to prepare solutions for film formation, a solvent common for both the ionic liquid and the polymer is crucial. Ionic liquids in general are soluble in polar organic solvents as acetone, methanol, and chloroform. Since the pristine PIM-1, PEG, copolymer PIM1_CO_2.5 and the ionic liquids [C_2mim][Tf_2N], [C_4mim][Tf_2N] and [C_6mim][Tf_2N] were all found to be soluble in chloroform, thus this solvent was used as a common solvent for blends formation. For preparing the blends, PIM-1 (5 wt.% with respect to the solvent) with ionic liquid [C_2mim][Tf_2N] or [C_4mim][Tf_2N] or [C_6mim][Tf_2N] (all 5 wt.% with respect to the PIM-1) were dissolved in chloroform in glass vials and stirred for one hour to form homogeneous and transparent solutions. The solutions were filtered and then poured onto a Teflon® mold that had been levelled. The solution in the mold was covered with a glass lid and purged with slow flow of N_2 overnight at room temperature. Such a drying technique ensured gradual removal of the solvent and thus limited the possibility of pin-hole formation in the membrane. The free standing films were further dried for 20 hours in a vacuum oven maintained at 65°C.

For blends of PIM-1 with PEG (2000 g/mol), PIM-1 and PEG (2.5 wt.% with respect to the PIM-1) were dissolved to form a homogeneous transparent solution. The ionic liquid [C_6mim][Tf_2N] (5 wt.% with respect to PIM-1), PIM-1 and PEG were all dissolved together in the common $CHCl_3$ to form a homogeneous solution.

The copolymer blends were also cast from $CHCl_3$ solutions in a manner similar to that of the aforementioned blends. The solution of ionic liquid [C_6mim][Tf_2N] in concentration of 2.5 wt.%, 5 wt.% and 10 wt.% (with respect to **PIM-COP**) was mixed with the copolymer solution in $CHCl_3$ and stirred for 2 hours until the formation of a clear solution. The films were cast at room temperature by drying in N_2 atmosphere and finally dried in a vacuum oven at 60°C for 24 hours.

2.5. Sample preparation for IL gas transport properties determination

In order to study gas transport properties of the ILs the membrane samples were prepared according to the method described elsewhere [33]. The 47 mm diameter Anodisk® membranes with 50 µm thickness were impregnated with IL and were used as porous membranes with highly reproducibility having a pore size (0.02 µm), pore size distribution close to unity and surface porosity (40±5%).

2.6. Characterization methods

2.6.1 Gel permeation chromatography (GPC)

GPC measurements were performed at room temperature in chloroform using a column combination [precolumn SDV-linear, SDV-linear and SDV-102 nm, with inner diameter 4.6mm and length 53cm, PSS GmBH, Mainz, Germany) at a flow rate of 1.0mL min^{-1}. A combination of refractive and UV detectors, with butylated hydroxy tolune as internal standard, was used for concentration detection. For evaluation of apparent molecular weight distribution, the universal PSS WinGPC software was used, based on calibration using PS standards.

2.6.2 ^{1}H Nuclear magnetic resonance (^{1}H-NMR)

NMR spectra were recorded on a Bruker AV500 NMR spectrometer (Germany) operating at a field of 7 Tesla (500 MHz) using a 5 mm ^{1}H/^{13}C TXI probe and a sample temperature of 25°C (298 K). ^{1}H spectra were recorded applying a 10 ms 90° pulse.

General equation for determining the concentration (wt.%) ionic liquid in the polymer blends from the NMR

$$\frac{W_{il}}{W_{all}} = \frac{n_{il} \times M_{il}}{(n_{il} \times M_{il}) + (n_{cp} \times M_{cp})} \quad (1)$$

where W_{il} , n_{il} and M_{il} are the weight, number of moles and molecular weight of the ionic liquid respectively

n_{cp} and M_{cp} correspond to the number of moles and molecular weight of the copolymer

W_{all} represents the weight of the entire blend composition

2.6.3 . Thermal gravimetric analysis (TGA)

A Netzsch TG209 F1 Iris (NETZSCH-Gerätebau GmbH, Selb, Germany) instrument was used to examine the decomposition temperature of the pure copolymer and the content of the residual solvent in the blends. The experiments were carried out in the temperature range 25°C - 900°C at a heating rate 10°C/min.

2.6.4 Water contact angle determination

A Kruss DSA100 drop shape investigator (Krüss GmbH, Hamburg,Germany) was used to conduct contact angle measurement studies. In order to investigate the contact angle a suitable drop needle diameter and the needle position were chosen to be 0.56 mm and S5 (manual), respectively. The computational analysis was done using the default water contact angle measurement program. A manual detection of the baseline was done before any angle was computed. De-ionized water was taken in a glass syringe and manually placed on the pure PIM-1 film during water contact angle measurements. In case of ionic liquids, the water in the syringe was replaced by the three different ionic liquids successively, and the average value of their contact angle on the pure PIM-1 film for the first 30 measurements was recorded. The measurement angles are an average of 20 measurements performed during the first 30 sec from left and right sides of the drop under ambient conditions.

2.6.5 Scanning electron microscopy (SEM) and energy dispersive X-ray analysis (EDX)

The morphology of membranes consisting of PIM-1, PIM-1 with ionic liquid, PIM-1-copolymer and PIM-1-copolymer with ionic liquid were studied using a Merlin microscope (Zeiss, Oberkochen, Germany). The microscope was equipped with an energy dispersive X-

ray analysis system (Oxford Instruments Nanoanalysis, Wiesbaden, Germany). Before investigating the surface and cross sections of the samples they were coated with carbon as a conductive layer. The cross section morphology was examined on cryogenically (liquid nitrogen) fractured samples. Elemental characterization was carried out in order to determine the spatial distribution of fluorine and sulfur as indicator for the ionic liquid.

2.6.6Density measurement

The density of the prepared membranes were determined by the buoyancy method as described elsewhere [34]As the immersion fluid the FC-77 perfluorinated liqud (3M, USA) was used as having least possible affinity to any component of the membrane. The density was calculated according to the Eqn. 2. The specific volume of the copolymer and the blends were calculated from the reciprocal of their densities.

Density of sample = $\frac{A}{A-B}(\rho_{o-}\rho_L) + \rho_L$ (2)

where A = weight of the sinker in air

B = weight of the sinker in displaced liquid

ρ_o = density of displaced liquid, FC-77 = 1.78 gcm^{-3}

ρ_L = density of air = 0.0012 gcm^{-3}

2.6.7 Gas transport measurement

An in-house designed “time lag” facility utilizing constant volume variable pressure approach was used for the determination of permeability, diffusion and solubility coefficients at 30°C and 500 mbar feed pressure. Each gas measurement was repeated 3 times to verify the results. The order of the gases during the measurement of one membrane sample was O_2, N_2, CO_2, N_2, CH_4, and N_2. Multiple N_2 measurements were carried out in order to ensure the stability of the membrane’s properties during the experiments and the absence of influence of highly soluble CO_2 on gas transport properties.

Similar to many other separation processes the solution diffusion model [35] can be applied in investigating the gas separation properties of our copolymer blends. According to this model, the permeant gas first gets adsorbed on the top side of the membrane, then diffusion of the penetrant through the free volume elements of the membrane takes place and finally there is desorption of the penetrant from the permeate side of the membrane.

The permeability (P), diffusion (D), solubility (S) coefficients and selectivity ($\alpha_{x/y}$) for gases x and y were determined under steady state by the following equations:

$$P = D*S = \frac{V_p l (P_{p2} - P_{p1})}{ART\Delta t(p_f - (p_{p2} + p_{p1}))} \quad (3)$$

$$D = \frac{l^2}{6\theta} \quad (4)$$

$$\alpha_{x/y} = \frac{P_x}{P_y} = \frac{D_x S_x}{D_y S_y} \quad (5)$$

where V_p is the constant permeate volume, R is the gas constant, l is the film thickness, A is the effective area of membrane, Δt is the time for the permeate pressure increase from p_{p1} to p_{p2}, p_f is the feed pressure and theta (θ) is the time lag.

For the determination of the gas transport properties of the ILs the corresponding Anodisk® supported IL membrane was placed and sealed in the measurement cell of the "time-lag" facility and evacuated until no trace of the desorption from the membrane was observed. The gas transport determination experiment was carried out according to the procedure described above. The permeability coefficients were corrected for the surface porosity of the Anodisk®.

2.6.8 Gas sorption experiment

CO_2 sorption of the pure copolymer and its blends were assessed by a gravimetric sorption ISOSORP magnetic suspension balance (Rubotherm GmBH, Bochum,Germany). The ISOSORP system is equipped with a precision pressure sensor DPI 282, with an accuracy of ± 0.006 bar. The adsorption measurements for all the blends were done and evaluated using a method as described elsewhere [36]. Before each measurement, the samples were evacuated overnight ($P \leq 10^{-6}$ mbar), to remove all residual volatile compounds that might remain dissolved. The balance was then thermostated to the temperature of measurement (30°C). The sorption measurements were conducted with pure gases of the 4.5 grade at a temperature of 30°± 0.1°C and in a pressure range 0.01 - 20 bar. The equilibrium weight was reached in approximately three hours after pressure change. For each gas, the measurements were conducted stepwise from vacuum up to a maximum pressure of 20 bar. The mass of the sample was corrected to take into account the buoyancy in the gas. Furthermore, the density measurements were performed following the Archimedes' principle, using the standard equipment for excellence Plus Mettler Toledo analytic balance (Germany). A non-swelling agent for PIM-1, copolymers and ILs, Fluorinert™ FC-77 was used as the fluid displaced by the sample. The real gas behavior was taken into account, the density of CO_2 and fugacity was determined using the chemical process optimization software Aspen Plus.

3. Results and Discussion

To achieve a better compatibility with the ionic liquid, instead of PIM-1, PIM-1/PEG blends and a copolymer of PIM-1 was synthesized. The copolymer contained 2.5 mol% of the hydrophilic PEG based anthracene maleimide comonomer (**CO**). Due to the step growth polymerization mechanism a random distribution of the hydrophilic comonomer along the chains can be assumed.

3.1 Synthesis of comonomer CO

The synthesis of the new comonomer (**CO**) is a three step reaction as shown in Figure 2 with a slight modification to a reported procedure [37]. In the first step, the tetramethoxy anthracene was readily prepared from the condensation reaction between pentanal and 1,2-dimethoxy benzene. The choice of the butyl group in the aldehyde was made to achieve enhanced solubility of the resulting compound. In the second step, the demethylation of tetramethoxy anthracene derivative was carried out to obtain the tetrahydroxy anthracene derivative. The anthracene maleimide derivative **CO** was prepared in the third step by Diels-Alder reaction between maleimide and anthracene derivative. The choice of such a monomer was made due to two reasons, firstly, the hydrophilicity of the PEG chain in the comonomer should help tune the polarity of the polymer and secondly, ethylene oxide units provide good CO_2 solubility due to the affinity of the hydrophilic ether towards quadrupolar gas CO_2 [38].

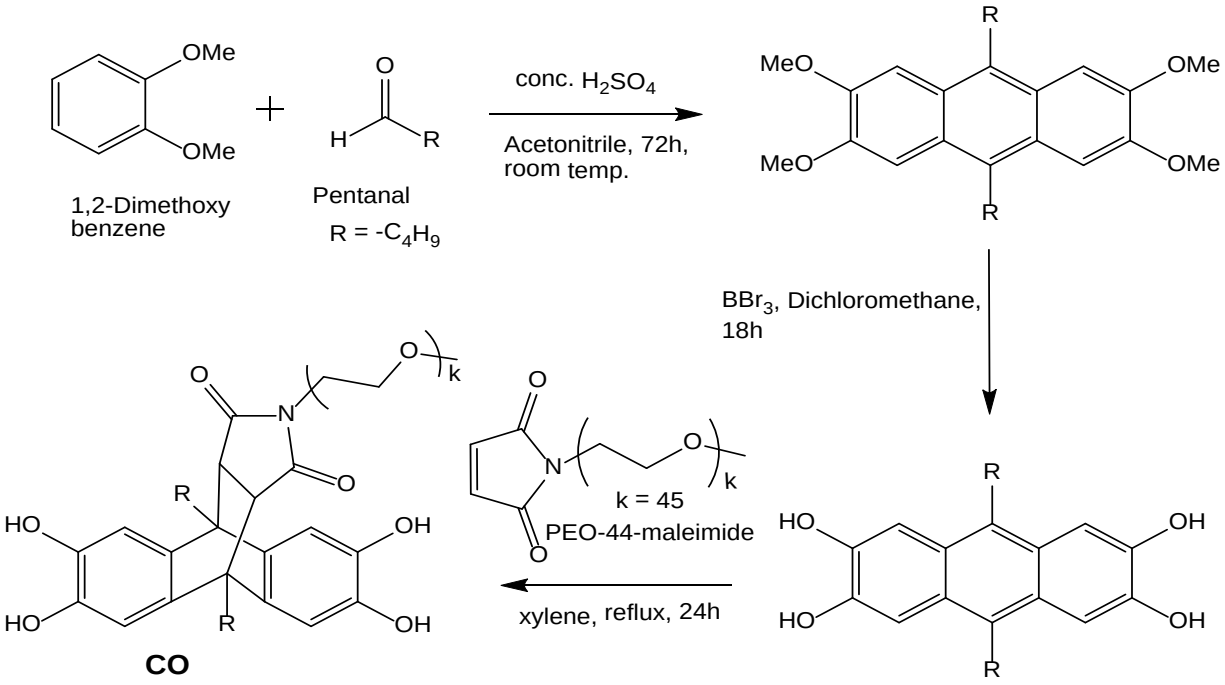

Figure 2**.** Synthesis of the new comonomer CO

The ^{1}H NMR spectra of **CO** is shown in Fig. 3. The four hydroxyl protons are observed at 8.67 and 8.72 ppm because they are deshielded. This is partly due to the electron withdrawing effect of the electronegative oxygen atoms and partly due to the delocalized electron cloud of the neighboring aromatic ring. The four aromatic protons are shifted downfield and appear at 6.65 and 6.73 ppm. Both the aromatic and hydroxyl protons are split due to the non-symmetric environment. The strong signal at 3.5 ppm represents the aliphatic protons of the PEG. The characteristic protons originating from the maleic anhydride also appear downfield at 3.13 ppm due to the proximity of the imide C═O, while the aliphatic protons of the butyl group can be observed in the range from 1.07 to 2.15 ppm.

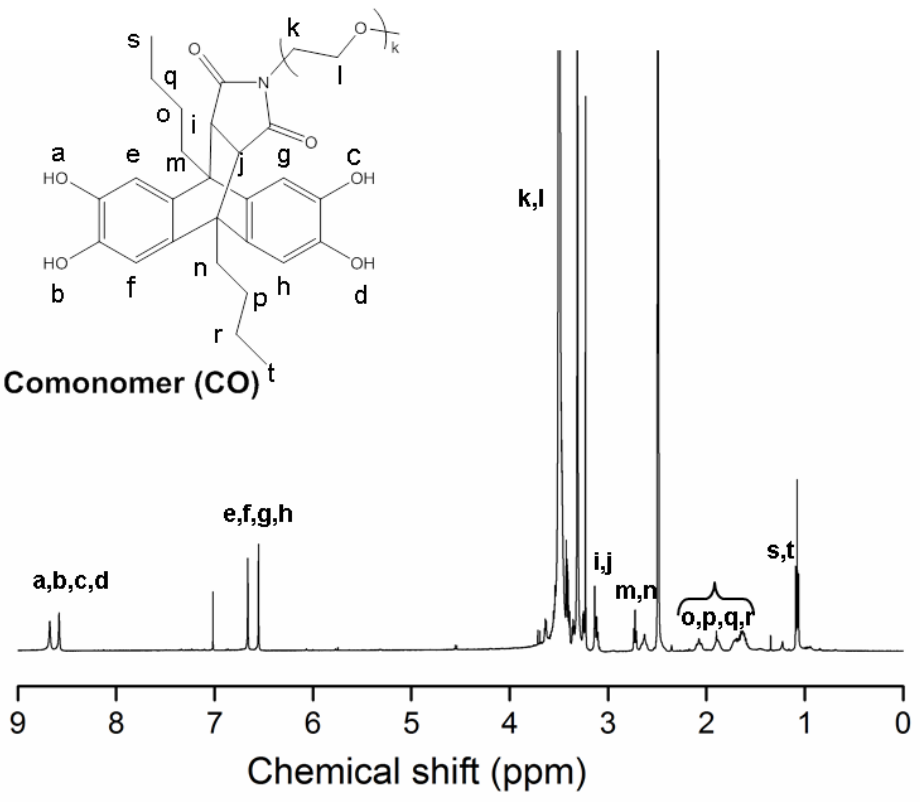

Figure 3**.** ^{1}H NMR spectrum of the new comonomer **CO** (in DMSO-d6).

3.2 Copolymer (PIM-COP) synthesis

PIM-COP was synthesized via polycondensation by reacting the tetrahydroxy monomer TTSBI and the comonomer (**CO**) in the ratio of (97.5:2.5) with equimolar amounts of TFTPN, catalyzed by an excess of K_2CO_3 (Fig. 4). The presence of PEG in the monomer made it essential to carry out the synthesis of the copolymer (**PIM-COP**) using the slow method[12]. Compared to the fast method of PIM-1 synthesis, the slow method used the double volume of solvent and was accomplished at a lower temperature. A series of trial polymerizations were conducted with the **CO** for polymerization time periods varying from 3 up to 15 days. The polymerizations running less than 15 days yielded low molecular weight copolymers, which did not produce stable membranes. The copolymer with the highest molecular weight ($1.23x10^5$ (g/mol) was used as the matrix for blends with 2.5, 5 and 10 wt.% $[C_6mim][Tf_2N]$. The novelty of such a copolymer is that it retains the PIM-1 characteristics (film forming) and gains hydrophilic character already at a low amount of only 2.5 mol% of the new comonomer (TTSBI:CO = 97.5:2.5 mol. %). The roof shaped structure of the anthracene maleimide moiety leads to an inefficient chain packing and hence should lead to lower permeability but improved selectivity.

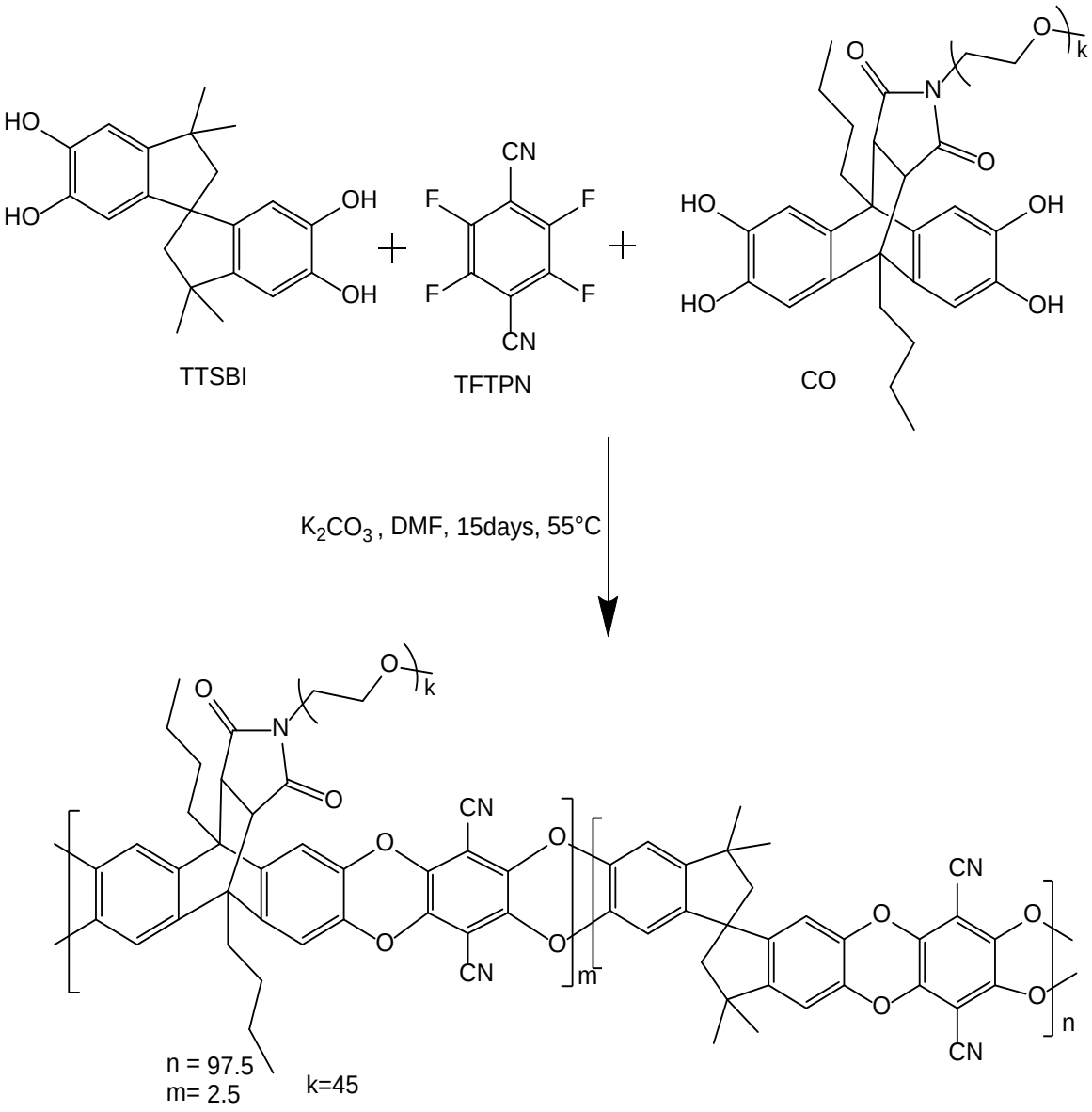

Figure 4**.** Synthesis of copolymer **PIM-COP**

Fig. 5 shows the ^{1}H NMR spectrum of the **PIM-COP** with allocation of protons. A major peak at 3.2 ppm is characteristic for the -OCH_2 protons of the PEG. The positions of the aromatic protons at 6.4 and 6.8 ppm and those of the aliphatic protons at 1.3 and 2.3 ppm are identical to pristine PIM-1[39]. Since the comonomer (**CO**) concentration was too low compared to the concentration of **TTSBI**, its corresponding aliphatic and aromatic protons could not be in detected in the ^{1}H NMR spectrum.

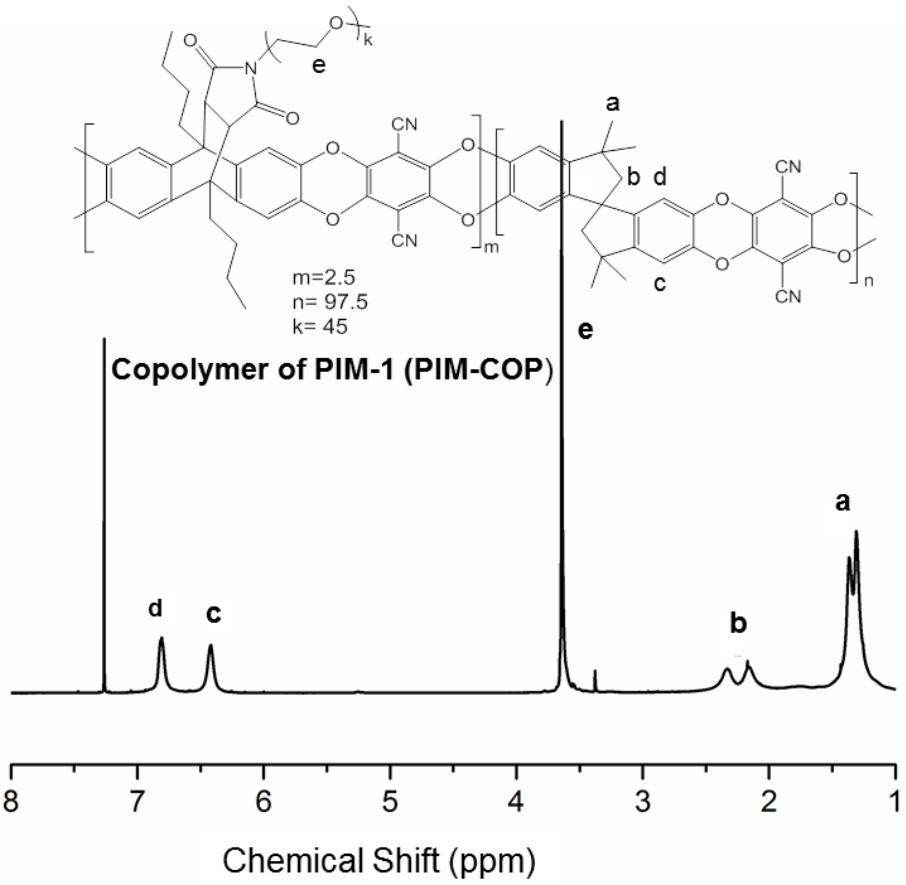

Figure 5. ^{1}H NMR spectrum of copolymer (**PIM-COP**) (in $CDCl_3$)

3.3 Characterization of blend membranes

3.3.1 Contact angle measurements

3.3.1.1 Ionic liquid contact angles on PIM-1

Since the major fraction of the synthesized copolymer and the PIM-1/PEG blend is PIM-1 it was important to determine the best suited ionic liquid for the distribution in the PIM-1 matrix. In the publication [33] the contact angle measurements were carried out to determine the ionic liquid most compatible with the poly(4-vinylpyridine) (P4VP). In another work [40]the interfacial behavior such as the wettability of the polymer by the IL has been ascertained by the determination of the contact angles of a broad range of ILs on polar and nonpolar substrates. Similar to the above works, a series of contact angle measurements with three different ionic liquids [C_2mim][Tf_2N], [C_4mim][Tf_2N], [C_6mim][Tf_2N] were conducted to determine the best compatibility with PIM-1. The smallest contact angle was found for the [C_6mim][Tf_2N] indicating that the IL with the longest alkyl chain forms the best blend with the PIM-1.

3.3.1.2 Water contact angle measurements on PIM-1, PIM1/PEG-2k-2.5 and PIM-COP

In order to check the improvement in hydrophilicity, the water contact angle of the PIM-1/PEG blend and the copolymer was compared with the pristine PIM-1 film. It was found that the water contact angle decreased to a larger extent for the copolymer than the blend (Fig. 6) implying that the copolymerization had a stronger influence in tuning the surface property of PIM-1 towards higher hydrophilicity.

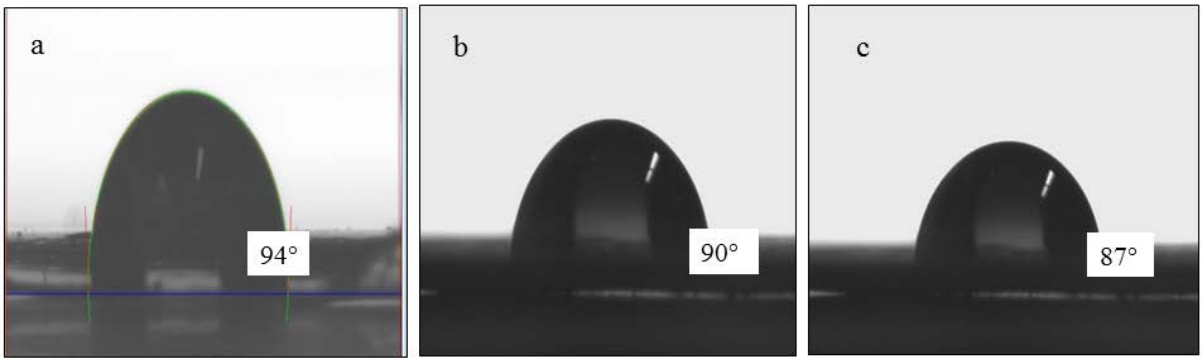

Figure 6. The sessile drop water contact angle on (a) PIM-1,(b) PIM-1/PEG 2k-2.5 and (b) **PIM-COP**

3.3.2. Blend morphology

Distribution of ionic liquid in PIM-1, PIM-1/PEG 2k-2.5 and PIM-1-COP

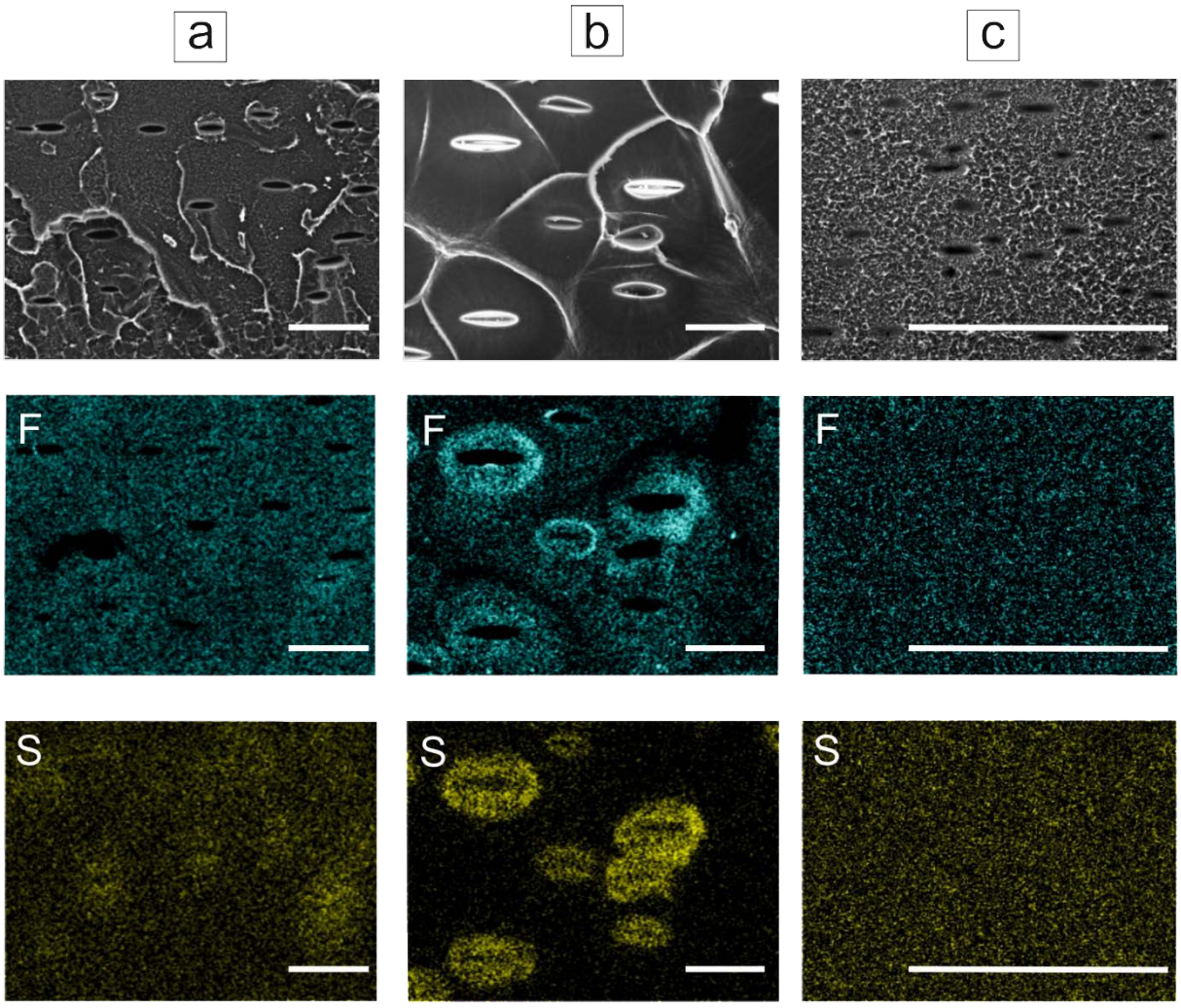

Figure 7. Secondary electron images of the cross section of (a) PIM-1 +5 wt.% IL, (b) PIM-1/PEG 2k-2.5 + 2.5 wt.% IL and (c) **PIM-COP** + 5 wt.% IL . Below are the X-ray maps from fluorine (F) and sulfur (S). All scale bars correspond to 10µm.

Fig. 7 shows the cross section morphology of PIM-1 + 5 wt.% IL, PIM-1/PEG 2k-2.5 + 2.5 wt.% IL and **PIM-COP** + 5 wt.% IL respectively, and the corresponding X-ray maps of fluorine and sulfur, which indicate the distribution of IL in the polymer. From Fig. 7a we find a completely irregular distribution of F and S in the pure PIM-1 suggesting a strong incompatibility between the hydrophobic PIM-1 and the relatively hydrophilic ionic liquid [C_6mim][Tf_2N]. In Fig. 7b the IL mixed with the PIM-1/PEG 2k-2.5 blend is presented. We find the localized distribution of ionic liquid centered only along the regions of the PEG, attributing dissolution of the IL only by the polar PEG regions of the blend. PEG is immiscible with PIM-1 and therefore segregated in domains, together with the IL. A strong phase separation or heterogeneity was observed only with 2.5 wt.% IL, therefore a blend with higher concentration of IL was not prepared.

However, for the copolymer of PIM-1 with the PEG containing comonomer (PIM-COP) (Fig. 7c), the F and S maps show a rather continuous distribution of ionic liquid even with 5 wt.% IL in the blend. This indicates a good compatibility of the ionic liquid with the copolymer. On the basis of the water contact angle and scanning electron microscopy tests it was established that the copolymer of PIM-1 (**PIM-COP**) forms the best blend with the IL .Further characterization was done with the blends of copolymer with varied contents of IL (2.5, 5 and 10wt% [C_6mim][Tf_2N] respectively).

3.4 Characterization of PIM-COP blend membranes

3.4.1 Thermal gravimetric analysis (TGA)

The TGA gives valuable information on the presence of volatile components in the sample under study and thedecomposition temperature of individual materials in the blend. Fig. 8 shows the TGA curve of the pure copolymer (**PIM-COP**), pure IL-[C_6mim][Tf_2N] and the blend [**PIM-COP** + [C_6mim][Tf_2N] membranes. For the pure copolymer, an initial loss in weight up to 250°C is found which might be due to the presence of residual solvent trapped in the membrane. Such weight loss as described in [41] is due to the polar PEG functionality introduced in the copolymer. In order to extract the residual solvent which can have specific interaction with the polymer it is a general practice to treat the film prepared by casting in a non-solvent e.g. methanol or ethanol. This practice is usual for investigation of gas transport properties of polyimides and PIMs [42]. In the current study which involved preparation and investigation of the polymer-IL blend materials it was considered as inappropriate to treat prepared membranes with any organic solvent which can be able to dissolve the IL and thus change the composition of the prepared material. Between 300°C and 400°C the further loss in weight can be attributed to the decomposition of the PEG chains constituting the copolymer along with the blends. Beyond 400°C the pure copolymer shows thermal stability up to almost 480°C, above which the maleimide groups of the comonomer starts to decompose due to the Retro Diels-Alder reaction. In case of the pure ionic liquid, we find that there is no loss in weight until it reaches its degradation point (380°C), indicating no traces of volatile solvents remaining trapped in the pure ionic liquid. The TGA pattern for all the blends is found to be identical to that of the pure copolymer, establishing that the ionic liquid incorporation does not bring about any major changes in the thermo-stability of the blends. For all the blend compositions there is an initial weight loss from 90°C to 100°C which is due to residual solvent remaining trapped in the membrane. However, since this loss is found only in the blends and not in the copolymer, it can be assumed that the presence of ionic liquid enhances

the tendency of the membranes to absorb surrounding moisture during the slow evaporation of the solvent. For the blends with 2.5 and 5 wt.% IL there is not much significant weight loss until 380°C, where it reaches the decomposition temperature of the ionic liquid. In case of the blend with 10 wt.% IL, there is a noticeable decrease in weight even below 350°C due to the excess ionic liquid incorporated in the copolymer. Above 350°C, there is a greater loss in weight than for the 2.5 and 5wt% blend compositions, respectively.

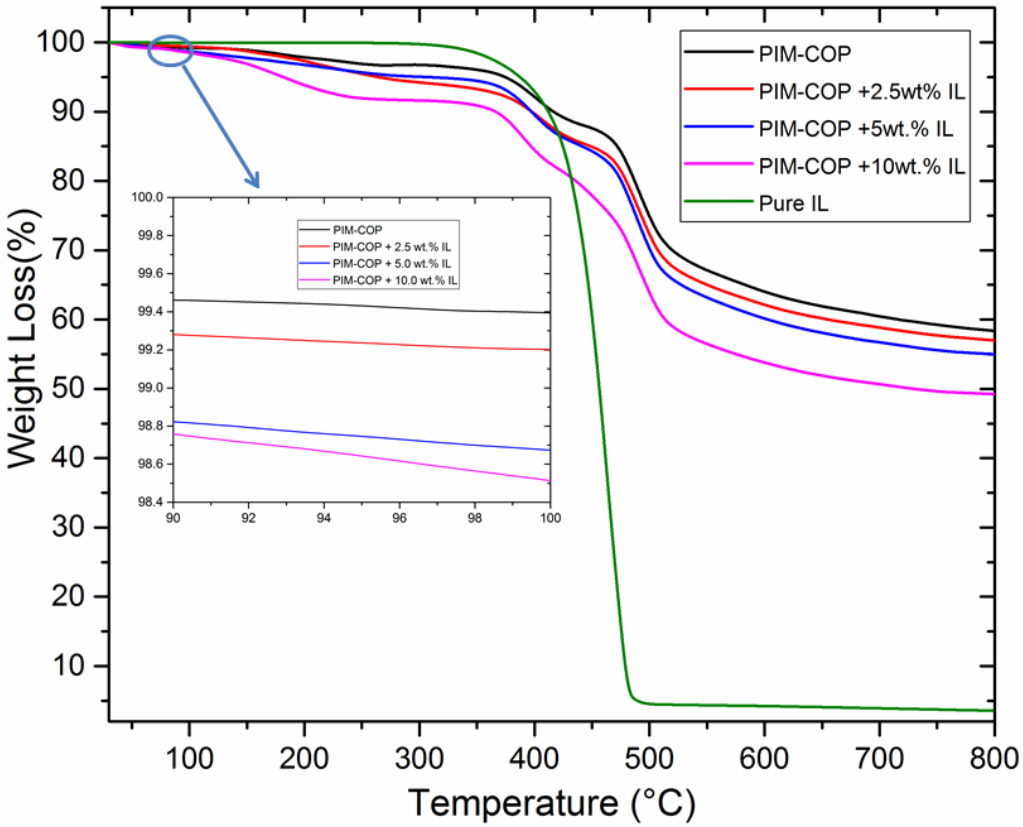

Figure 8. TGA curve of **PIM-COP** and the blends of **PIM-COP** with varied contents of the IL (2.5, 5 and 10wt.% [C_6mim][Tf_2N]). In the inset, the weight loss of the blends from 90°C-100°C has been displayed.

3.4.2 ^{1}H-NMR

The stacked ^{1}H NMR (Fig. 9) spectra was used to determine the percentage composition of the IL incorporated in the sample. This additionally confirmed that no IL was pressed out from the blends.

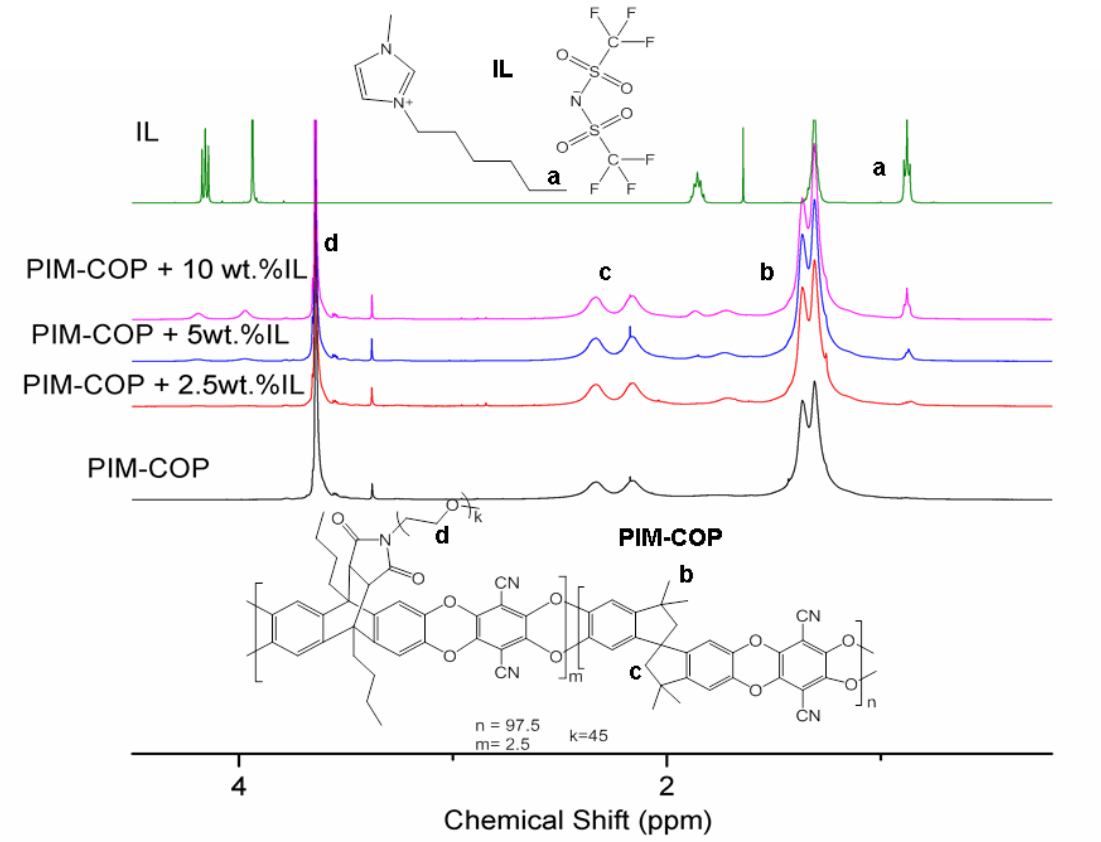

Figure 9. The stacked ^{1}H NMR spectra of IL, **PIM-COP** and blends of **PIM-COP**/IL (measured in $CDCl_3$)

Table 1. Comparison of the weighed in wt.% of [C_6mim][Tf_2N] (experimental) with the corresponding values obtained by ^{1}H-NMR integrals (calculated) in the polymer blends

Membrane	Experimental (wt.%)	Calculated (wt.%)
1. PIM-COP + 2.5 wt.% IL	2.5	5.0
2. PIM-COP + 5.0 wt.% IL	5.0	7.5
3. PIM-COP + 10 wt.% IL	10.0	13.0

The values from ^{1}H-NMR integrals are calculated from equation (1) provided in Section 2.6.2

3.4.3 Effect of the amount of ionic liquid content on PIM-COP morphology

The backscattered electron images of the cross sections of the copolymer and its blends with 2.5, 5 and 10 wt.% of ionic liquid are shown in Fig. 10. Ellipsoidal domains can be observed, which become more and larger with increasing content of ionic liquid in the blend. The ellipsoidal shape is due to sample preparation. The IL agglomerates and forms bigger domains in the blend with higher content of the IL[43]. The formation of such agglomerates occurs due to phase separation in the copolymer matrix and influences the gas permeation properties as will be discussed later

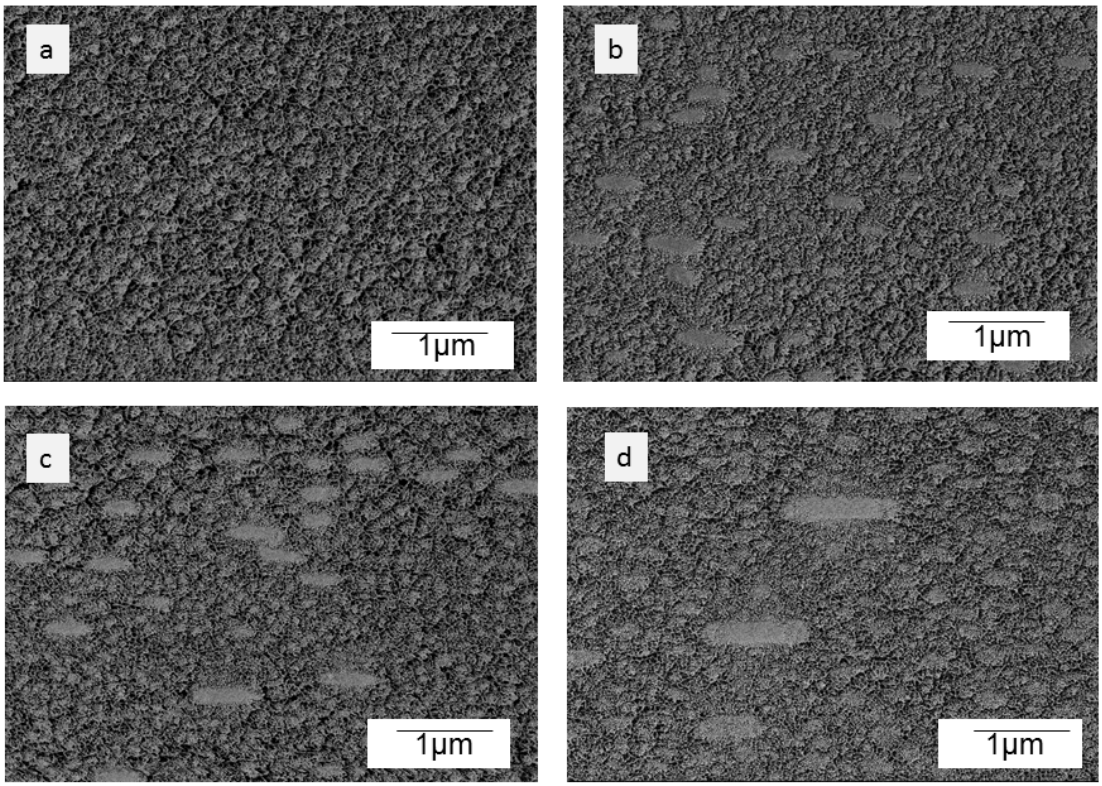

Figure 10. SEM backscattered electron images of (a) pure **PIM-COP** (b) blend **PIM-COP** + 2.5wt.% [C_6 mim][Tf_2N] (c) blend **PIM-COP** + 5.0wt.% [C_6mim][Tf_2N], (d) blend **PIM-COP** + 10.0wt.% [C_6 mim][Tf_2N]. Accelerating voltage: 900eV

3.5 Gas transport measurements

3.5.1 Effect of IL on properties of the PIM-1 based blends

The gas permeation characteristics were studied for PIM-1 based blends containing the same amount (5wt.%) of [C_2mim][Tf_2N], [C_4mim][Tf_2N] and[C_6mim][Tf_2N]. The permeability coefficients of CO_2, N_2, CH_4, O_2 and the ideal gas selectivities of some important gas pairs are provided in Table 2. It was found that as the length of the alkyl chain in the incorporated IL increases from [C_2mim][Tf_2N] to [C_6mim][Tf_2N], the quantity of elliptical ionic liquid

domains in the PIM-1 matrix increases and, consequently, disturbs the permeation of gases, causing the permeability of all gases to decrease. Although there is an increment of gas solubility in the blend brought about by the longer alkyl chains [44], its contribution to the overall permeability is diminished by the formation of low permeable morphological features in the blend membrane.

Table 2. Gas permeabilities and selectivity of various gas pairs in pure PIM-1 and blends of PIM-1+5 wt.%[C_2mim][Tf_2N], PIM-1+5 wt.%[C_4mim][Tf_2N] and PIM-1+5wt.%[C_6mim][Tf_2N]

1 Barrer = $1x10^{-10}$ cm^3(STP) cm $cm^{-2}s^{-1}cmHg^{-1}$

Membrane	Permeability (Barrer)				Selectivity		
	CO_2	N_2	CH_4	O_2	CO_2/N_2	CO_2/CH_4	O_2/N_2
PIM-1	7440	397	652	1130	19	11	2.8
PIM-1+5wt%[C_2mim][Tf_2N]	6650	332	593	1040	20	11	3.1
PIM-1+5wt%[C_4mim][Tf_2N]	4590	212	349	701	22	13	3.3
PIM-1+5wt%[C_6mim][Tf_2N]	2240	90	165	310	25	14	3.4

Consequently, there is gradual enhancement of gas pair selectivity for CO_2/N_2, CO_2/CH_4 and O_2/N_2 with the increase in the length of the alkyl chain. Both the observation of decrease of permeability and increase of selectivity of the blends of PIM-1 /IL with the increase in cation size, are in disagreement with previously reported data [45], according to which, with the increase in the alkyl chain length in the ionic liquid, there is substantial increase of the fractional free volume of the polymer/IL blend which cause the overall permeability to increase and selectivity to decrease due to the contributing diffusivity term. It can be concluded that the non-consistency in the gas permeability and selectivity data for the pristine PIM-1 and its blends with ionic liquids arises from the lack of compatibility of [C_2mim][Tf_2N] , [C_4mim][Tf_2N] and [C_6mim][Tf_2N] with hydrophobic PIM-1. In parallel, the adsorption of the the hydrocarbon tails of the IL into the high free volume of the polymer can also be considered as a reason for the decrease of permeability and increase of selectivity for the PIM-1/IL blends.

3.5.2 Effect of IL content on properties of the copolymer based blends

The newly synthesized **PIM-COP** shows significantly lower permeability coefficients for all gases compared to the pure PIM-1. The permeability decrease is represented by the sequence: N_2 (5.16 times) > CH_4 (4.93 times) > O_2 (4.66 times) >CO_2 (3.96 times) and is a function of decreasing diffusivity. Additionally, since the permeability decrease is not fitting to the line of kinetic diameter changes for these penetrants, it can be indicated that for the **PIM-COP** membrane the solubility of gases also plays a role.. Consequently, the selectivity of the copolymer differs from the PIM-1 as well: while the CO_2/N_2 selectivity is significantly increased, both O_2/N_2 and CO_2/CH_4 selectivities have changed to a lesser extent. The CO_2/CH_4 selectivity increased while the O_2/N_2 selectivity decreased. It is interesting to observe that the O_2/N_2 selectivity of the copolymer is very low, even significantly lower than that of the PEG based block-copolymers Pebax® 1657 or PolyActive™ 1500 [36] indicating that significant rearrangement of the free volume of the glassy polymer should occur upon addition of the comonomer with a long PEG side chain. Addition of the ionic liquid into the copolymer leads to further decrease of permeability coefficients. The effect of $[C_6mim][Tf_2N]$ content on the **PIM-COP** matrix was investigated by the incorporation of 2.5, 5 and 10 wt.% of IL and studying single gas permeation characteristics of resulting blends. The density, the permeability of CO_2, N_2, CH_4, O_2 and the selectivities of some important gas pairs for the **PIM-COP** based blends having different content of the $[C_6mim][Tf_2N]$ are shown in Table 3. The gas permeabilities were found to follow the same trend as those for the pure PIM-1 membranes: $CO_2 > O_2 > CH_4 > N_2$ [46] (Table 3).

Table 3. Density, single gas permeabilities, and selectivities of various gas pairs in copolymer of PIM-1(PIM-COP), and blends of PIM-COP+2.5 wt.%$[C_6mim][Tf_2N]$, 5 wt.%$[C_6mim][Tf_2N]$, and 10 wt.%$[C_6mim][Tf_2N]$

Membrane	Density (g/cm^3)	Permeability(Barrer)				Selectivity		
		CO_2	N_2	CH_4	O_2	CO_2/N_2	CO_2/CH_4	O_2/N_2
PIM-COP	1.13	1880	77	132	242	24	14	3.1
$[C_6mim][Tf_2N]$	1.37	610	25	55	90	24	11	3.7
PIM-COP+2.5 wt.%$[C_6mim][Tf_2N]$	1.14	970	37	56	148	26	16	4.0
PIM-COP+5 wt.%$[C_6mim][Tf_2N]$	1.16	900	33	53	113	28	17	3.4
PIM-COP+10 wt.%$[C_6mim][Tf_2N]$	1.21	812	27	43	101	30	19	3.7

1 Barrer = $1x10^{-10}$ cm^3(STP) cm $cm^{-2}s^{-1}cmHg^{-1}$

The density of the blend materials increased with the increased content of IL, however not proportional to the IL content. Unfortunately determination of the free volume for the blend of

polymer and ionic liquid which is just partially soluble in the polymer matrix is not a trivial task, since it is difficult to evaluate with an acceptable accuracy the occupied volume of the copolymer itself and that of the added ionic liquid which can be partially molecularly distributed in the polymer and partially forms a separate phase which was observed as ellipsoidal inclusions in the polymer matrix.

The permeabilities of all the gases were found to decrease as the content of the IL increased from 2.5 wt.% to 10 wt.% (Fig. 11). Already at 2.5 wt.% content of the IL in the copolymer matrix, a significant decrease of the permeability coefficients was observed for all studied gases and this decrease is not proportional to the change of the specific volume of the blend. At higher IL loading this change was not as drastic as upon addition of the first 2.5 wt.% of the IL and not as high as change of the specific volume. It indicates that only a limited quantity of the IL can be dissolved or dispersed on a molecular level in the polymer matrix, most probably in the free volume voids of the polymer thus effectively blocking gas transport pathways. The remaining, not molecularly dispersed, part of the IL forms elliptical elements in the bulk of the polymer matrix creating additional interfaces representing an obstacle for the passage of gas molecules. The selectivity of the blend did not change significantly depending on the content of the IL: the biggest selectivity increase is observed for gas pairs having high difference in kinetic diameters (CO_2/CH_4 and CO_2/N_2) while O_2/N_2 permeability selectivity was mostly intact.

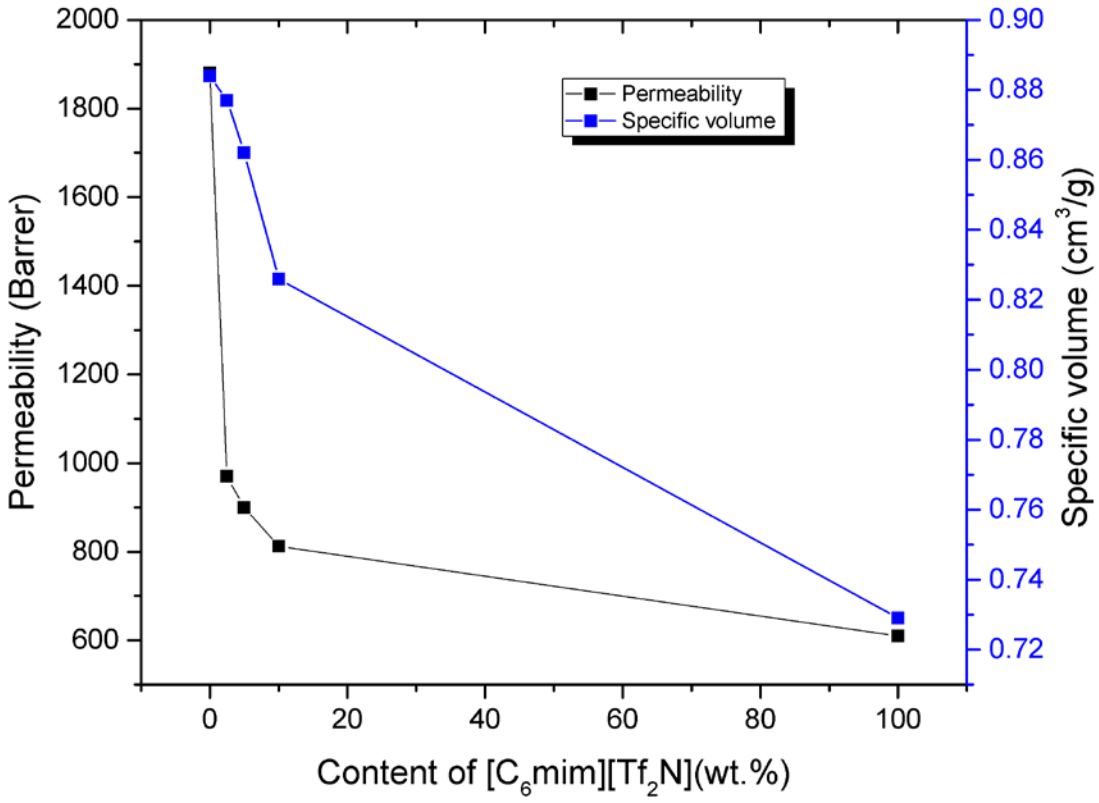

Figure 11. CO_2 Permeability and specific volume of the **PIM-COP**/IL blends at 30°C

To better understand the effects of IL on gas permeability in **PIM-COP**/IL blends, the contribution of solubility and diffusion coefficients to the overall blend permeability is demonstrated in Figs. 12 and 13, respectively. The solubility coefficient of CO_2 was found to increase significantly with the increment in the ionic liquid content. Both gases with high critical temperature, CO_2 and CH_4 show similar solubility coefficient increase compared to the pure copolymer while O_2 and N_2 having significantly lower critical temperatures show lower solubility increase compared to former two gases (Fig. 12). This is quite an expected trend, since the solubility is a thermodynamic phenomenon and depends on the nature of the permeating gas and the interaction between the penetrant and the polymer [47]. Since [C_6mim][Tf_2N] has a high solubility specifically for CO_2 [31], thus the changes in concentration of IL does not change the solubility of other gases as much as of CO_2.

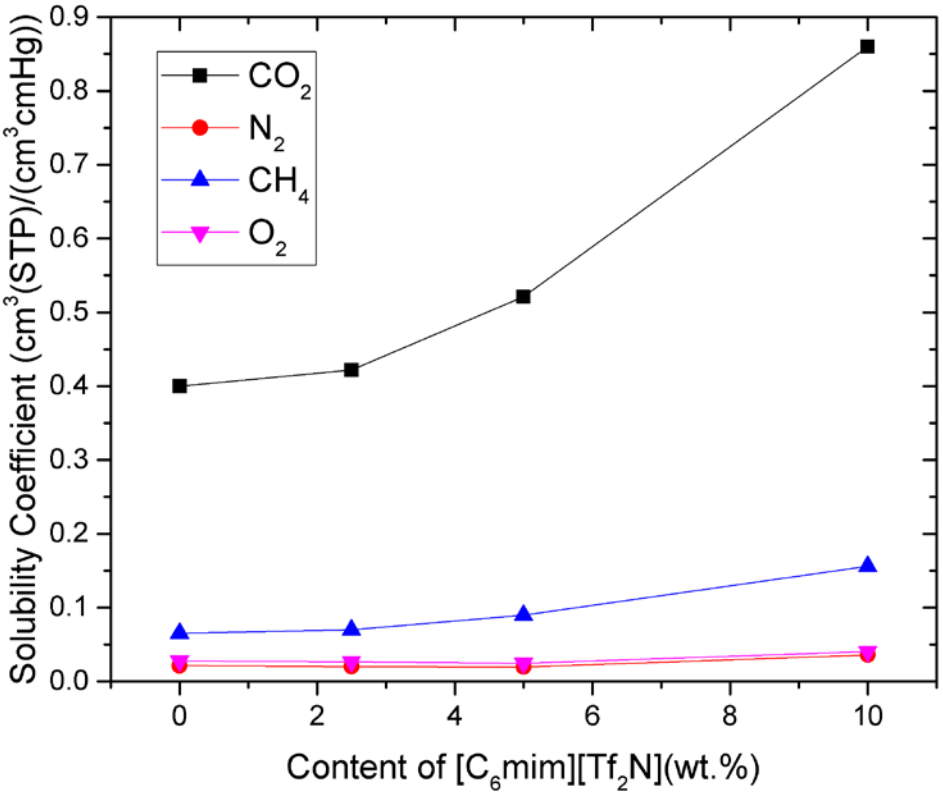

Figure 12**.** Solubility coefficients of blend membranes of **PIM-COP**+[C_6mim][Tf_2N] at 30°C determined by the time lag method

Furthermore, Fig. 13 demonstrates that the diffusion coefficients of CO_2, N_2, CH_4, and O_2 display a decreasing trend. The diffusion depends on size and shape of the penetrant and the fractional free volume (void size and voids interconnection) of the polymer matrix [48]. Being

a kinetic size dependent phenomenon, the diffusion coefficients of all gases are affected by introduction of the IL into the blend differently compared to the solubility coefficients. Among the gases having the trend of kinetic diameter increase as: $CO_2 < O_2 < N_2 < CH_4$, O_2 demonstrates the highest value of the diffusion coefficient among other studied gases, even the CO_2. Zhou *et al*. in their work based on a PIM-ethanoanthracene- Tröger's base membrane [49] have argued that the reason for such an ambiguity is due to two factors. Firstly, there is a strong interaction between CO_2 and the IL trapped in the membrane and secondly the linear shape of CO_2 might increase the resistance time in entering the void.

The diffusion coefficient for all gases is found to decrease with the increase of the IL content. The diffusion coefficients of CO_2 and O_2 are found to exhibit a similar trend and also N_2 and CH_4 are found to behave similar. However, the diffusion for all the gases is found to decrease drastically with the addition of 2.5 wt.% IL followed by a gradual or linear decrease for the blends with higher amounts of IL. It is important to mention that the diffusion coefficient dependence on IL content for all gases shows exactly the same behavior as the permeability coefficient which is decreasing significantly after addition of 2.5 wt.% of IL. This permeability decrease is a function of both the decrease of the diffusion coefficient and mostly intact solubility coefficient as it follows from the solution-diffusion model of transport through the polymeric media. Taking into account the combined effect of diffusivity and solubility, the permeability can be considered to be controlled mainly by diffusivity and thus the overall permeability of all the gases decreases.

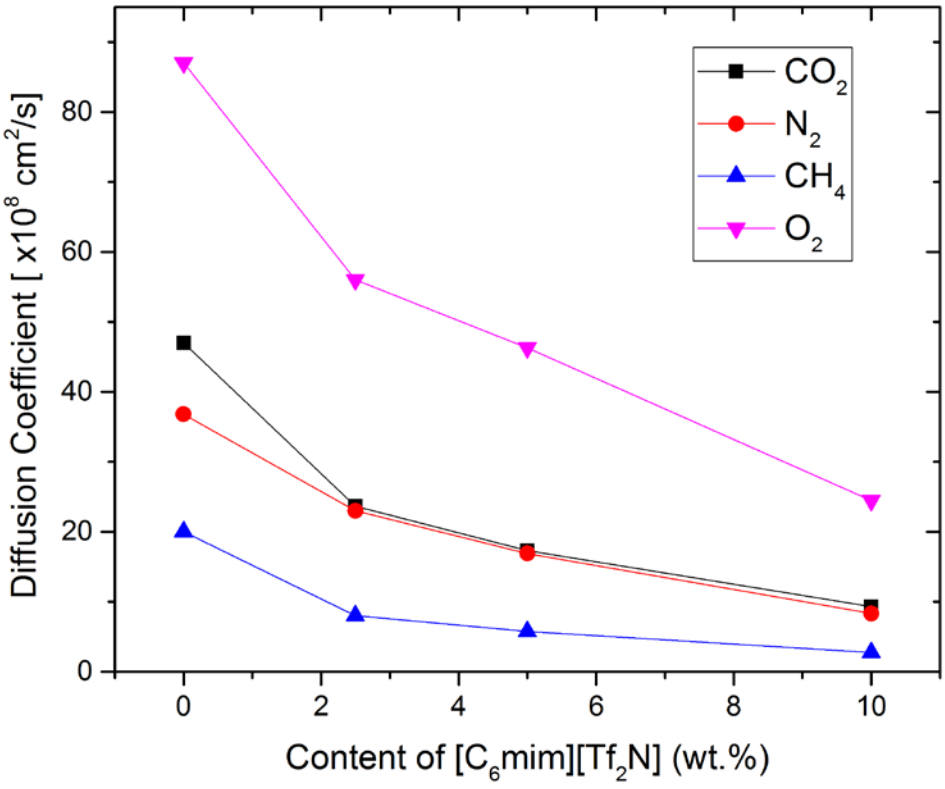

Figure 13**.** Diffusion coefficients of blend membranes of **PIM-COP** +[C_6mim][Tf_2N] at 30°C by the time lag method

Table 4. Solubility selectivity, diffusivity selectivity of CO_2/N_2, CO_2/CH_4 and O_2/N_2 gas pairs in copolymer of **PIM-COP**, and blends of **PIM-COP**+2.5 wt.%[C_6mim][Tf_2N], 5 wt.%[C_6mim][Tf_2N], and 10 wt.%[C_6mim][Tf_2N]

Membrane	Solubility selectivity		Diffusivity Selectivity	
	(CO_2/N_2)	(CO_2/CH_4)	(CO_2/N_2)	(CO_2/CH_4)
PIM-COP	18.60	6.13	1.31	2.32
PIM-COP + 2.5wt% [C_6mim][Tf_2N]	23.39	6.03	1.11	2.87
PIM-COP + 5wt% [C_6mim][Tf_2N]	26.71	5.64	1.02	3.00
PIM-COP + 10wt% [C_6mim][Tf_2N]	26.20	5.53	1.12	3.44

For the CO_2/N_2 gas pair, the solubility selectivity is found to increase with the increment of [C_6mim][Tf_2N] from 2.5 wt.% to 5 wt.%. In general the solubility selectivity of a penetrant in a polymer (thermodynamic phenomenon) at constant operating conditions (such as temperature, pressure and composition) is purely governed by penetrant condensability and

polymer-penetrant interactions [47]. The IL not only has a high solubility for the condensable CO_2 gas but also some molecular simulation analysis shows that, with the spherical $[Tf_2N]^-$ anion, the CO_2 can align tangentially, favoring strong interactions between the partial positive charge of carbon of CO_2 and partial negative charge on the fluorine atoms of the anion [50]. The CO_2 specific interaction with the ionic liquid trapped in the free volume cavity of the copolymer causes the solubility selectivity for the CO_2/N_2 to increase. But for the blend with 10 wt.% IL, the solubility selectivity decreases a bit because the major part of the dispersed ionic liquid no longer accommodates in the free volume cavities of the copolymer, but it is rather distributed in-homogeneously in the phase separated medium causing the interaction of $[C_6mim][Tf_2N]$ to be less specific towards CO_2. The CO_2/N_2 diffusivity selectivity, however, remains almost constant for all the blend compositions due to similar diffusivities of the two gases. In the case of the CO_2/CH_4 gas pair, in addition to their different diffusivities (Fig. 14) the large kinetic diameter of CH_4 causes its diffusion coefficient to be more strongly affected (decreased) than the diffusion coefficient of CO_2. This improves the overall diffusivity selectivity of CO_2/CH_4. But unlike the solubility selectivity of CO_2/N_2, the solubility selectivity of CO_2/CH_4 is found to remain roughly stable. This observation fits the explanation given by Ramdin et al. [51] where the non-polar CH_4 gas experiences a boost in solubility due to the addition of the non-polar hexyl chain originating from the cation of the ionic liquid. The mentioned paper discusses that while the solubility of CO_2 is dominated by free volume effects, the solubility of CH_4 is dominated by nonpolar-non dispersive interactions. Therefore due to the increase of both CO_2 and CH_4 solubilities the $[C_6mim][Tf_2N]$ is not able to enhance CO_2/CH_4 solubility selectivity significantly. Therefore the permselectivity increase of CO_2/N_2 (Fig. 14) is mostly controlled by the solubility selectivity, while for the CO_2/CH_4 pair the diffusivity selectivity plays the more vital role.

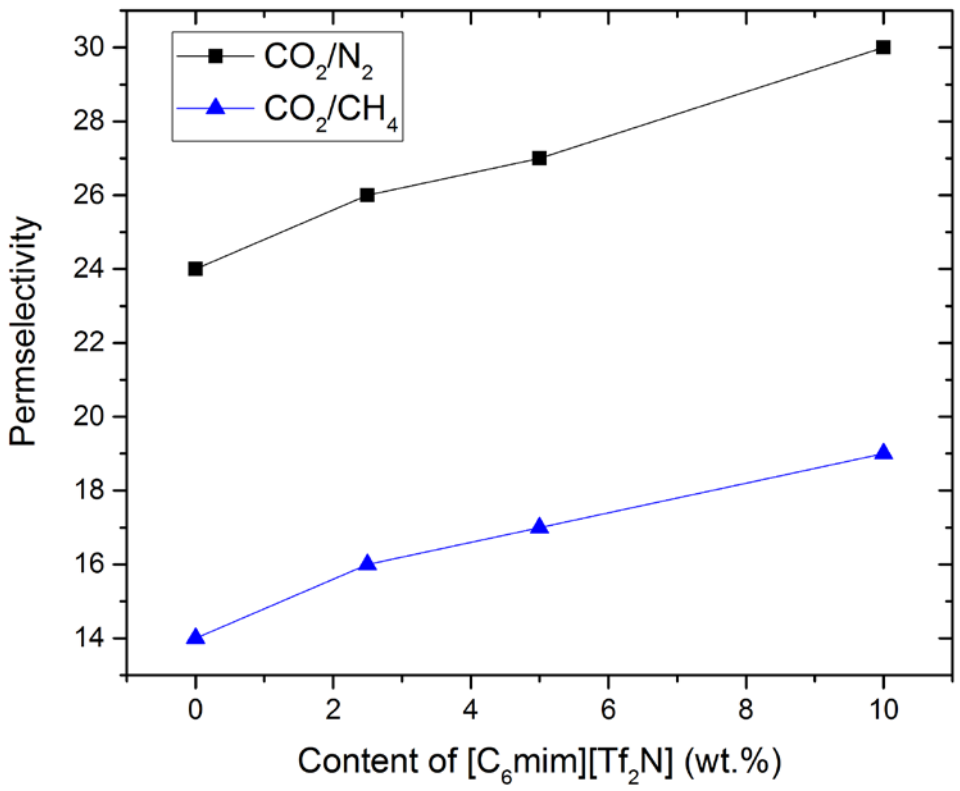

Figure 14. Effect of [C_6mim][Tf_2N] content on the selectivity of CO_2 /N_2 and CO_2 /CH_4 for the blends of PIM-COP + 2.5 wt.%, 5 wt.% and 10 wt.% ionic liquid

The reason for the higher selectivity of the [C_6mim][Tf_2N]+copolymer blends can be attributed to the directed channels created by the ionic liquid sections distributed throughout the blend matrix. The scanning electron microscope images (Fig. 10) confirm the formation of islands in the matrix of the copolymer with the increase in the content of the [C_6mim][Tf_2N], thus facilitating the selective passage of CO_2 throughout the blend. Thus the addition of [C_6mim][Tf_2N] could be very useful where high CO_2/N_2 selectivity with moderate permeability is required.

3.6 Maxwell model simulation of permeability and density

Since the SEM images (Section 3.4.3) reveal a heterogeneous character of the blends, the Maxwell model was used to describe the gas transport properties of the blend membranes. The Maxwell model for heterogeneous blends can be expressed as [52]

$$P_{eff} = P_c \left[\frac{P_d + 2P_c - 2\emptyset_d (P_c - P_d)}{P_d + 2P_c + \emptyset_d (P_c - P_d)}\right] \quad (6)$$

where P_{eff} is the effective permeability, P_c and P_d are the permeabilities of the continuous and the dispersed phase in the blend membrane, respectively. The Maxwell model in this system continuously estimates the property of a two component system in the full range of concentrations. In our

case, the higher permeable copolymer is considered as the continuous phase and the IL is considered as the dispersed phase. However, the CO_2 permeability for the heterogeneous blends (Fig. 15) calculated by Eqn. 6 was found to be mostly linearly dependent on the amount of IL in the blend membrane in the whole range of compositions and higher than the permeability of our blend systems.

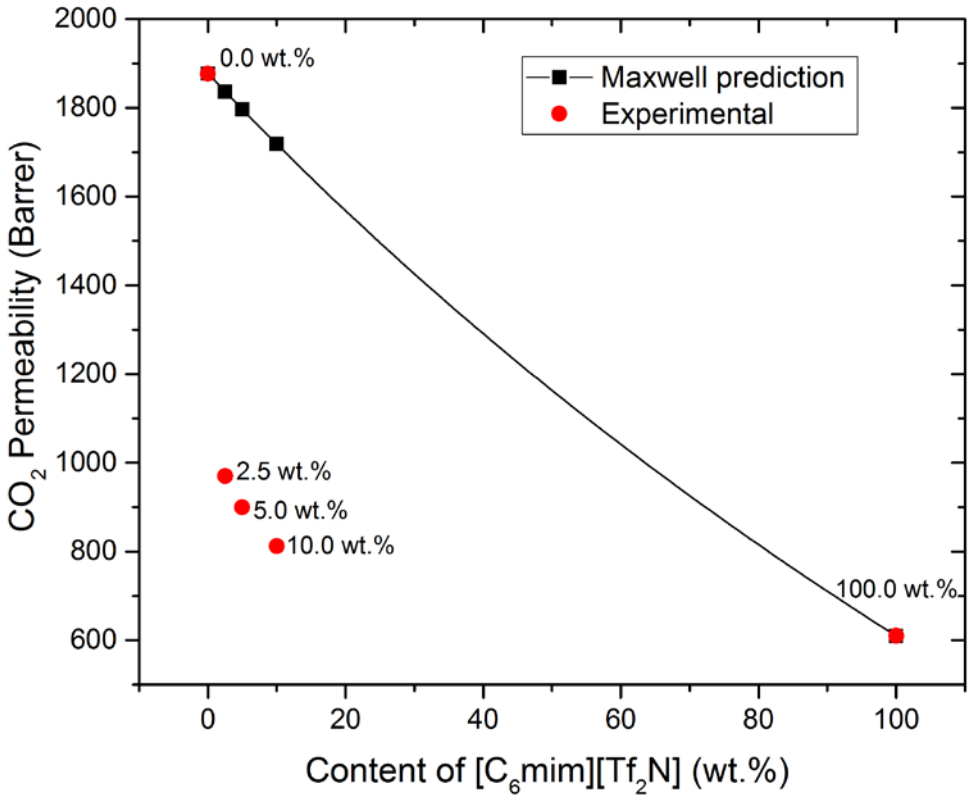

Figure 15. Comparison between (calculated) Maxwell permeability and the experimental permeability of the **PIM-COP**/IL blends

This behavior can be explained by the partial miscibility of the blends' components and localization of IL molecules in the free volume elements of the polymer matrix provoking diffusion pathway blocking and hence reduction of the gas permeability. The difference in permeability between the experimental and theoretical values gets more pronounced as the concentration of IL in the blend increases. It can be assumed that for higher concentration of IL, the molecular level interactions get superseded by the IL molecules agglomeration

forming discontinuous phase of IL and thus increasing the tortuosity of the gas molecules path through the polymer.

In [53], an increase of CO_2/H_2 selectivity by the addition of PEG into the PEBAX matrix, was attributed to the fractional free volume(FFV) change in the membrane matrix. Since the FFV can be related to their densities, a comparison of the experimental densities with the values obtained by the additive model has been made. In the current work, since a correlation between the specific volume and permeability has been made (Fig 11), hence the Maxwell model is considered for an effective comparison of the experimental densities with those of the theoretical values. The density of the **PIM-COP**/IL blend according to the Maxwell model changes linearly with the IL content while the experimentally determined density follows the predicted line only for the blend with 2.5 wt.% IL and drastically deviates from the predicted value at higher IL concentrations (Fig. 16). This observation is in good agreement with the gas transport data visualizing the limited solubility or molecular level distribution of the IL in the polymer matrix. At low IL content most of the IL is distributed in the free volume of the polymer causing effective blocking of the diffusion pathways. When the IL concentration exceeds the miscibility level between 2.5 and 5 wt.%, the density starts to increase more significantly than it can be expected from the Maxwell model prediction but the gas permeability does not decrease proportionally to this density change clearly indicating the effect of additional tortuosity for the gas diffusion due to appearance of IL phase in the polymer matrix. Significant increase of the density for the blends with 5 and 10 wt.% IL can arise from the formation of polymer/IL interface which has properties different from the bulk polymer.

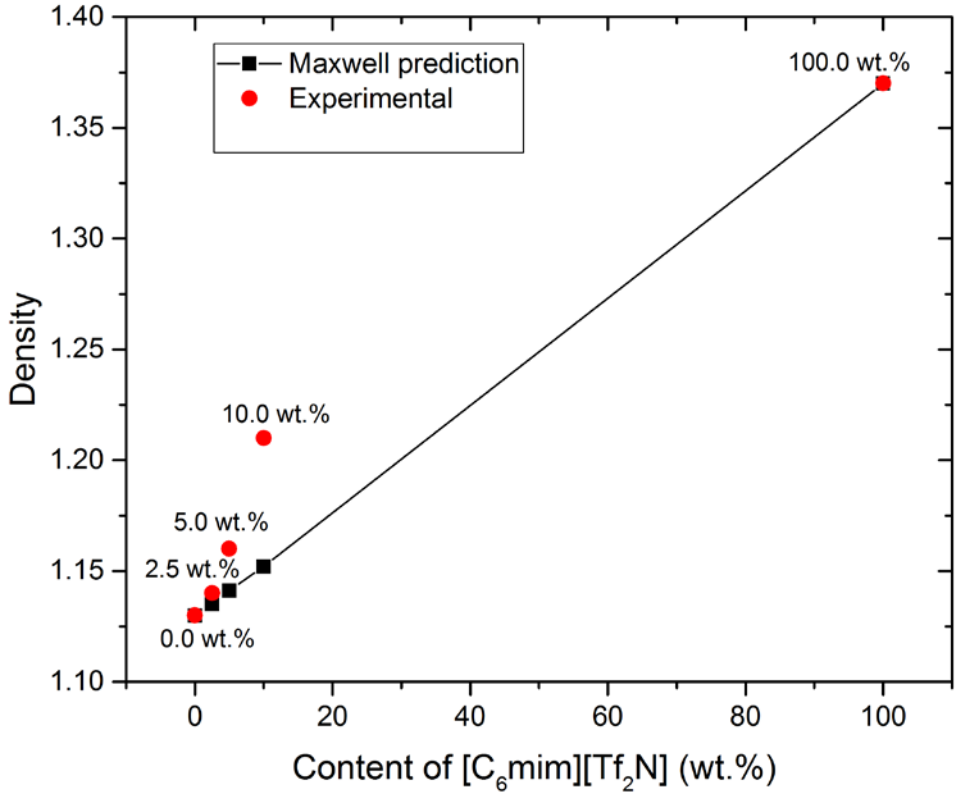

Figure 16. Comparison of the Maxwell density and the experimental density of **PIM-COP**/IL blends.

It was found that the density of our blends is higher than predicted from the Maxwell model. This is possible when the blends are miscible and there is a linear increase in the density with the increase in the IL content. However the deviations get larger when compared to the blends having a higher IL content. Combining the results from permeability and density values it can be predicted that the blends are partially miscible.

3.7 Sorption Measurement

A study of the transient and equilibrium sorption of condensable species over the entire vapor activity range in the pure **PIM-COP**, pure [C_6mim][Tf_2N], and the blend membranes of **PIM-COP**, was performed by sorption measurements (Fig. 17). The sorption behavior of the pure copolymer follows the dual mode sorption model [54] which assumes that two concurrent modes of sorption pertaining to the polymer sites are operative in a heterogeneous medium. Either the penetrant is normally dissolved and is responsible for diffusion (like the sorption in rubbery polymers) or there is an immobilization of the penetrant fractions on constant energy

sites or microvoids in the polymer (characteristic of glassy polymers). Therefore, the initial uptake which is rapid and is a linear function of pressure follows Henry's law (due to the part involved in diffusion), while in the latter part the sorption curve approaches a quasi-equilibrium followed by a slow approach due to the saturation capacity of the fixed sites (Langmuir isotherm due to the immobilized fraction). The affinity of the copolymer/IL blend for the CO_2 is provided by the low pressure region, whilst the effect of IL on the free volume and mobility of the PIM-1 chains or swelling accompanied by the condensability of the CO_2 is indicated by the high pressure region.

In case of the pure [C_6mim][Tf_2N], the sorption curve is found to follow the Henry's Law. Since the CO_2 adsorption for IL in general is a function of molar volume and length of the counter ion [33] the [C_6mim][Tf_2N] is found to possess a high CO_2 adsorption capacity at low pressure due to high molar volume and a significantly longer bis(trifluoromethylsulfonyl)imide counter anion [55]. In case of the blends, the condensability of CO_2 accompanied by the swelling of the copolymer chains leads to a very high CO_2 uptake [56].

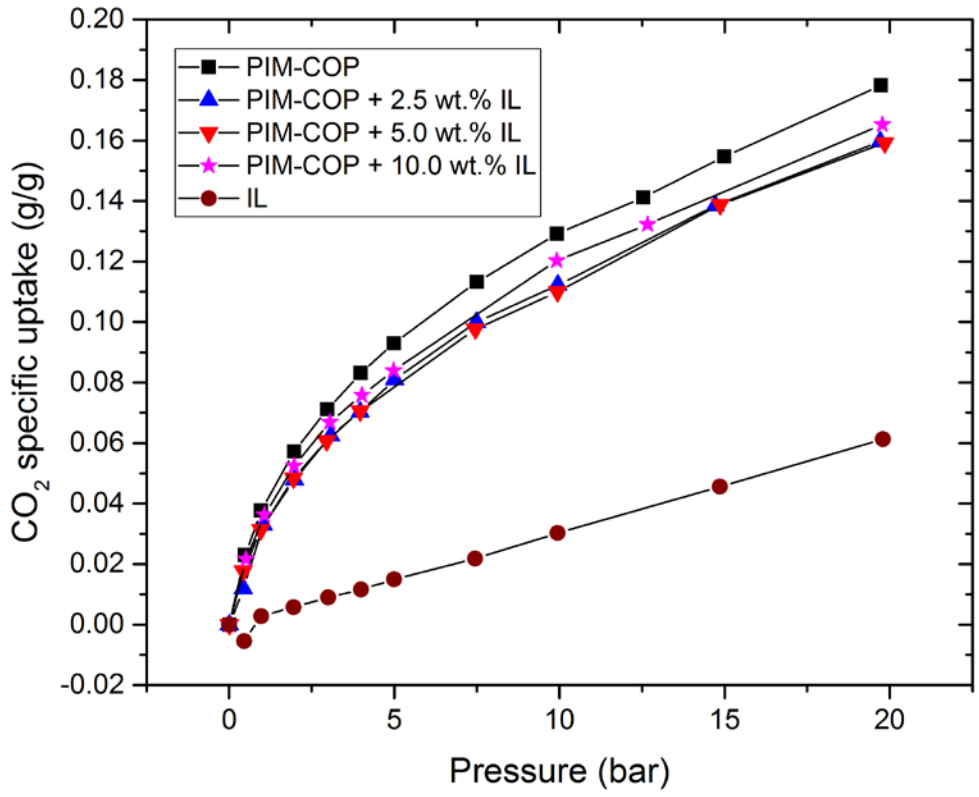

Fig 17. CO_2 sorption isotherms for different blend compositions and IL at 30°C

Comparing the sorption behavior for all compounds in the low pressure domain where the gas adsorbent interactions overcome the swelling effects, we find that all the blend compositions have lower uptake than the pure copolymer..

This result proves that since the dissolution of CO_2 in the copolymer and the blends is an equilibrium step, hence the specific uptake is not influenced by the gradual addition of the ionic liquid in the copolymer matrix. The increment in the specific uptake gets less pronounced with the further addition of ionic liquid. This can be explained by the filling of the free volume fraction in the copolymer by the ionic liquid and leaving lesser void spaces for the uptake of the penetrant.

The table of solubility coefficients obtained from the "Time-lag" experiment and from the gas sorption experiment at 1 bar pressure is prepared below for deeper understanding of gas transport properties of blend membranes

Table 5. CO_2 solubility coefficients at 1 bar pressure derived from the direct sorption and the Time-lag experiments

Membrane	CO_2 solubility at 1 bar pressure (pressure decay method) (cm^3(STP)/cm^3cmHg)	Solubility according to the time lag method (cm^3(STP)/cm^3cmHg)
PIM-1	0,46	0.80
PIM-COP	0.29	0.40
IL	0.026	0.019
PIM-COP + 2.5 wt% IL	0.24	0.42
PIM-COP + 5.0 wt% IL	0.25	0.52
PIM-COP + 10.0 wt% IL	0.27	0.80

As one can see from the solubility coefficients table there is relatively good correspondence of the values obtained for solid samples with the deviation ranging from 27% to 67 % for pure polymer and for polymer/IL blends. Generally, the solubility coefficient obtained indirectly via the S=P/D equation from the "Time-lag" experimental results is higher than that obtained from the gas adsorption experiment. The higher solubility values from the ''time lag'' method for the copolymer and the blends can be attributed to the fact that this method uses an inherently different measurement concept, where the experiments are finished in less than 20 seconds. However in the magnetic sorption balance (MSB) experiment or the pressure decay method, the dissolution of CO_2 in the copolymer and the blends is an equilibrium step, thus sorption values are obtained in longer time than the former method [33]. The values obtained for the IL show the opposite behavior where the solubility coefficient at 1 bar CO2 pressure from the absorption experiment is 37% higher than the "Time-lag" derived value. The

[C_6mim][Tf_2N] solubility value is in good agreement with the literature [57] and its lower magnitude compared to PIM-1 and PIM-COP can be explained by its low fractional free volume(FFV) as compared to polymers [58].

4. Comparison of gas separation performance

Previous works [59, 60] have investigated the use of ILs as ideal liquid phases for supported liquid membranes due to their low volatility and high thermal stability. In order to overcome the problem of long term stability in such supported liquid membranes (SLMs) free standing poly room temperature ionic liquids(RTILs) membranes have been fabricated with faster CO_2 sorption and better mechanical stability. However, gas diffusivity was reduced in poly(RTILs) due to restricted chain mobility after polymerization. Heterogeneous PVDF/[emim][BF_4] polymer gels [61]and PVDF/[emim][DCA] [29]exhibit better gas transport properties because ofthe absence of any molecular level interactions that might reduce gas permeability. Grünauer et al. [33] in their work have used isoporous poly(styrene-*block*-4-vinypyridine) PS-*b*-P4VP as the membrane matrix to accommodate ionic liquids for efficient gas separation SLMs. The regular surface porosity and self-organization behavior of PS-b-P4VP have been exploited in this work, to achieve long term stability of ionic liquids in the pore of the isoporous membrane. Ionic liquids have also been used as dopant on cellulose triacetate (CTA)[62], to reduce the crystallinity of the CTA and enhance its affinity with CO_2, leading to improvement in CO_2 permeability and CO_2/ light gas selectivity. However in the current work, the ionic liquid [C_6mim][Tf_2N] was used as a filler material in a dense PIM-COP matrix. Although the permeability decreased slightly, the improvement of CO_2/N_2 selectivity promises the use of the studied polymer-IL composites as selective layer materials in thin film composite membranes.

5. Conclusions

Blend membranes of the ionic liquid [C_6mim][Tf_2N] embedded in a chemically modified polymer of intrinsic microporosity were successfully prepared. The ionic liquid [C_6mim][Tf_2N] was chosen for its high CO_2 solubility and relatively hydrophobic character

induced by the hexyl chain in the cation. A tuning of PIM-1 polarity was found to be essential to achieve compatibility of the polymer and [C_6mim][Tf_2N]. Copolymerization of PIM-1 was done with a new PEG containing comonomer based on anthracene maleimide (**CO**). The SEM investigation, especially of secondary electron images of the cross section of the copolymer blends, and water contact angle measurements proved the better compatibility of the copolymer **PIM-COP** with [C_6mim][Tf_2N]. The single gas permeation data of the copolymer blend improved CO_2/N_2 selectivity compared to pure PIM-1. Lowering of the CO_2 permeability coefficient from 7440 Barrer for PIM-1 down to approximately 800 Barrer for the blend resulted in the permeability selectivity for CO_2/N_2 to increase from 19 to 30 (determined at 30°C).

Acknowledgement

The authors would like to thank Silke Dargel, Silvio Neuman, Joachim Koll, Anke-Lisa Metze for their technical support, Dr. Jelena Lillepärg for the sorption measurements and Dr. Gisela Bengtson for helpful discussions. This work was financially supported by the Helmholtz Association for the German Research Centres through the Helmholtz Portfolio MEMBRAIN.

References.

[1] M. Buonomenna, W. Yave, G. Golemme, Some approaches for high performance polymer based membranes for gas separation: block copolymers, carbon molecular sieves and mixed matrix membranes, RSC Advances, 2 (2012) 10745-10773.
[2] L. Hao, K.-S. Liao, T.-S. Chung, Photo-oxidative PIM-1 based mixed matrix membranes with superior gas separation performance, Journal of Materials Chemistry A, 3 (2015) 17273-17281.
[3] M.M. Khan, G. Bengtson, S. Shishatskiy, B.N. Gacal, M.M. Rahman, S. Neumann, V. Filiz, V. Abetz, Cross-linking of polymer of intrinsic microporosity (PIM-1) via nitrene reaction and its effect on gas transport property, European Polymer Journal, 49 (2013) 4157-4166.
[4] L.M. Robeson, The upper bound revisited, Journal of Membrane Science, 320 (2008) 390-400.
[5] P. Pandey, R. Chauhan, Membranes for gas separation, Progress in Polymer Science, 26 (2001) 853-893.
[6] G. Maier, Gas separation with polymer membranes, Angewandte Chemie International Edition, 37 (1998) 2960-2974.
[7] P.M. Budd, N.B. McKeown, Highly permeable polymers for gas separation membranes, Polym. Chem., 1 (2010) 63-68.

[8] A.P. Cote, A.I. Benin, N.W. Ockwig, M. O'Keeffe, A.J. Matzger, O.M. Yaghi, Porous, crystalline, covalent organic frameworks, science, 310 (2005) 1166-1170.
[9] A.I. Cooper, Conjugated microporous polymers, Advanced Materials, 21 (2009) 1291-1295.
[10] M. Calle, C.M. Doherty, A.J. Hill, Y.M. Lee, Cross-linked thermally rearranged poly (benzoxazole-co-imide) membranes for gas separation, Macromolecules, 46 (2013) 8179-8189.
[11] Y.P. Yampolskii, Amorphous perfluorinated membrane materials: structure, properties and application, Russian Journal of General Chemistry, 79 (2009) 657-665.
[12] P.M. Budd, E.S. Elabas, B.S. Ghanem, S. Makhseed, N.B. McKeown, K.J. Msayib, C.E. Tattershall, D. Wang, Solution-processed, organophilic membrane derived from a polymer of intrinsic microporosity, Advanced Materials, 16 (2004) 456-459.
[13] N.B. McKeown, P.M. Budd, K.J. Msayib, B.S. Ghanem, H.J. Kingston, C.E. Tattershall, S. Makhseed, K.J. Reynolds, D. Fritsch, Polymers of intrinsic microporosity (PIMs): bridging the void between microporous and polymeric materials, Chemistry–A European Journal, 11 (2005) 2610-2620.
[14] N.B. McKeown, P.M. Budd, Polymers of intrinsic microporosity (PIMs): organic materials for membrane separations, heterogeneous catalysis and hydrogen storage, Chemical Society Reviews, 35 (2006) 675-683.
[15] N.B. McKeown, P.M. Budd, Exploitation of intrinsic microporosity in polymer-based materials, Macromolecules, 43 (2010) 5163-5176.
[16] A. Gonciaruk, K. Althumayri, W.J. Harrison, P.M. Budd, F.R. Siperstein, PIM-1/graphene composite: A combined experimental and molecular simulation study, Microporous and Mesoporous Materials, 209 (2015) 126-134.
[17] N. Du, G.P. Robertson, J. Song, I. Pinnau, M.D. Guiver, High-performance carboxylated polymers of intrinsic microporosity (PIMs) with tunable gas transport properties, Macromolecules, 42 (2009) 6038-6043.
[18] C.R. Mason, L. Maynard-Atem, N.M. Al-Harbi, P.M. Budd, P. Bernardo, F. Bazzarelli, G. Clarizia, J.C. Jansen, Polymer of intrinsic microporosity incorporating thioamide functionality: preparation and gas transport properties, Macromolecules, 44 (2011) 6471-6479.
[19] N. Du, H.B. Park, G.P. Robertson, M.M. Dal-Cin, T. Visser, L. Scoles, M.D. Guiver, Polymer nanosieve membranes for CO2-capture applications, Nature materials, 10 (2011) 372-375.
[20] N. Du, G.P. Robertson, J. Song, I. Pinnau, S. Thomas, M.D. Guiver, Polymers of intrinsic microporosity containing trifluoromethyl and phenylsulfone groups as materials for membrane gas separation, Macromolecules, 41 (2008) 9656-9662.
[21] M.M. Khan, V. Filiz, T. Emmler, V. Abetz, T. Koschine, K. Rätzke, F. Faupel, W. Egger, L. Ravelli, Free Volume and Gas Permeation in Anthracene Maleimide-Based Polymers of Intrinsic Microporosity, Membranes, 5 (2015) 214-227.
[22] F.Y. Li, Y. Xiao, T.-S. Chung, S. Kawi, High-performance thermally self-cross-linked polymer of intrinsic microporosity (PIM-1) membranes for energy development, Macromolecules, 45 (2012) 1427-1437.
[23] W. Yong, F. Li, Y. Xiao, P. Li, K. Pramoda, Y. Tong, T. Chung, Molecular engineering of PIM-1/Matrimid blend membranes for gas separation, Journal of membrane science, 407 (2012) 47-57.
[24] D. Paul, S. Newman, Polymer blends, vol. 2, Academic, New York, (1978).
[25] G. Guerrica-Echevarria, J. Eguiazabal, J. Nazabal, Partially miscible blends based on a polyarylate and poly (trimethylene terephthalate), Journal of applied polymer science, 92 (2004) 1559-1561.
[26] X.M. Wu, Q.G. Zhang, P.J. Lin, Y. Qu, A.M. Zhu, Q.L. Liu, Towards enhanced CO 2 selectivity of the PIM-1 membrane by blending with polyethylene glycol, Journal of Membrane Science, 493 (2015) 147-155.
[27] E.L. Cussler, Diffusion: mass transfer in fluid systems, Cambridge university press, 2009.
[28] J. Holbrey, K. Seddon, Ionic liquids, Clean Products and Processes, 1 (1999) 223-236.
[29] H.Z. Chen, P. Li, T.-S. Chung, PVDF/ionic liquid polymer blends with superior separation performance for removing CO 2 from hydrogen and flue gas, International journal of hydrogen energy, 37 (2012) 11796-11804.

[30] L. Liang, Q. Gan, P. Nancarrow, Composite ionic liquid and polymer membranes for gas separation at elevated temperatures, Journal of Membrane Science, 450 (2014) 407-417.
[31] J.L. Anderson, J.K. Dixon, J.F. Brennecke, Solubility of CO_2, CH4, C2H6, C2H4, O2, and N2 in 1-Hexyl-3-methylpyridinium Bis (trifluoromethylsulfonyl) imide: Comparison to Other Ionic Liquids, Accounts of chemical research, 40 (2007) 1208-1216.
[32] N. Du, J. Song, G.P. Robertson, I. Pinnau, M.D. Guiver, Linear High Molecular Weight Ladder Polymer via Fast Polycondensation of 5, 5', 6, 6'-Tetrahydroxy-3, 3, 3', 3'-tetramethylspirobisindane with 1, 4-Dicyanotetrafluorobenzene, Macromolecular Rapid Communications, 29 (2008) 783-788.
[33] J. Grünauer, S. Shishatskiy, C. Abetz, V. Abetz, V. Filiz, Ionic liquids supported by isoporous membranes for CO/N2 gas separation applications, Journal of Membrane Science, (2015).
[34] M.M. Rahman, J. Lillepärg, S. Neumann, S. Shishatskiy, V. Abetz, A thermodynamic study of CO 2 sorption and thermal transition of PolyActive™ under elevated pressure, Polymer, 93 (2016) 132-141.
[35] J. Wijmans, R. Baker, The solution-diffusion model: a review, Journal of membrane science, 107 (1995) 1-21.
[36] M.M. Rahman, J. Lillepärg, S. Neumann, S. Shishatskiy, V. Abetz, A thermodynamic study of CO 2 sorption and thermal transition of PolyActive™ under elevated pressure, Polymer, (2016).
[37] M.M. Khan, G. Bengtson, S. Neumann, M.M. Rahman, V. Abetz, V. Filiz, Synthesis, characterization and gas permeation properties of anthracene maleimide-based polymers of intrinsic microporosity, RSC Advances, 4 (2014) 32148-32160.
[38] H.W. Kim, H.B. Park, Gas diffusivity, solubility and permeability in polysulfone–poly (ethylene oxide) random copolymer membranes, Journal of Membrane Science, 372 (2011) 116-124.
[39] B. Satilmis, P.M. Budd, Base-catalysed hydrolysis of PIM-1: amide versus carboxylate formation, RSC Advances, 4 (2014) 52189-52198.
[40] M.M. Pereira, K.A. Kurnia, F.L. Sousa, N.J. Silva, J.A. Lopes-da-Silva, J.A. Coutinho, M.G. Freire, Contact angles and wettability of ionic liquids on polar and non-polar surfaces, Physical Chemistry Chemical Physics, 17 (2015) 31653-31661.
[41] G. Wang, Y. Weng, D. Chu, D. Xie, R. Chen, Preparation of alkaline anion exchange membranes based on functional poly (ether-imide) polymers for potential fuel cell applications, Journal of Membrane Science, 326 (2009) 4-8.
[42] Y. Yampolskii, A. Alentiev, G. Bondarenko, Y. Kostina, M. Heuchel, Intermolecular interactions: new way to govern transport properties of membrane materials, Industrial & Engineering Chemistry Research, 49 (2010) 12031-12037.
[43] M.M. Khan, V. Filiz, G. Bengtson, S. Shishatskiy, M. Rahman, V. Abetz, Functionalized carbon nanotubes mixed matrix membranes of polymers of intrinsic microporosity for gas separation, Nanoscale research letters, 7 (2012) 1-12.
[44] S.H. Lee, S.B. Lee, The Hildebrand solubility parameters, cohesive energy densities and internal energies of 1-alkyl-3-methylimidazolium-based room temperature ionic liquids, Chemical communications, (2005) 3469-3471.
[45] M.G. Cowan, M. Masuda, W.M. McDanel, Y. Kohno, D.L. Gin, R.D. Noble, Phosphonium-based poly (Ionic liquid) membranes: The effect of cation alkyl chain length on light gas separation properties and Ionic conductivity, Journal of Membrane Science, 498 (2016) 408-413.
[46] S. Thomas, I. Pinnau, N. Du, M.D. Guiver, Pure-and mixed-gas permeation properties of a microporous spirobisindane-based ladder polymer (PIM-1), Journal of Membrane Science, 333 (2009) 125-131.
[47] D.F. Sanders, Z.P. Smith, R. Guo, L.M. Robeson, J.E. McGrath, D.R. Paul, B.D. Freeman, Energy-efficient polymeric gas separation membranes for a sustainable future: a review, Polymer, 54 (2013) 4729-4761.
[48] B.D. Freeman, Basis of permeability/selectivity tradeoff relations in polymeric gas separation membranes, Macromolecules, 32 (1999) 375-380.
[49] J. Zhou, X. Zhu, J. Hu, H. Liu, Y. Hu, J. Jiang, Mechanistic insight into highly efficient gas permeation and separation in a shape-persistent ladder polymer membrane, Physical Chemistry Chemical Physics, 16 (2014) 6075-6083.

[50] T. Cremer, C. Kolbeck, K.R. Lovelock, N. Paape, R. Wölfel, P.S. Schulz, P. Wasserscheid, H. Weber, J. Thar, B. Kirchner, Towards a Molecular Understanding of Cation–Anion Interactions—Probing the Electronic Structure of Imidazolium Ionic Liquids by NMR Spectroscopy, X-ray Photoelectron Spectroscopy and Theoretical Calculations, Chemistry–A European Journal, 16 (2010) 9018-9033.
[51] M. Ramdin, S.P. Balaji, A. Torres-Knoop, D. Dubbeldam, T.W. de Loos, T.J. Vlugt, Solubility of Natural Gas Species in Ionic Liquids and Commercial Solvents: Experiments and Monte Carlo Simulations, Journal of Chemical & Engineering Data, 60 (2015) 3039-3045.
[52] J.C. Maxwell, A treatise on electricity and magnetism. Vol. 1, (2014).
[53] A. Car, C. Stropnik, W. Yave, K.-V. Peinemann, PEG modified poly (amide-b-ethylene oxide) membranes for CO2 separation, Journal of Membrane Science, 307 (2008) 88-95.
[54] W. Vieth, J. Howell, J. Hsieh, Dual sorption theory, Journal of Membrane Science, 1 (1976) 177-220.
[55] J. Palomar, V.R. Ferro, J.S. Torrecilla, F. Rodríguez, Density and molar volume predictions using COSMO-RS for ionic liquids. An approach to solvent design, Industrial & Engineering Chemistry Research, 46 (2007) 6041-6048.
[56] F. Jutz, J.-M. Andanson, A. Baiker, Ionic liquids and dense carbon dioxide: a beneficial biphasic system for catalysis, Chemical reviews, 111 (2010) 322-353.
[57] M. Gonzalez-Miquel, J. Bedia, J. Palomar, F. Rodriguez, Solubility and Diffusivity of CO2 in [hxmim][NTf2],[omim][NTf2], and [dcmim][NTf2] at T=(298.15, 308.15, and 323.15) K and Pressures up to 20 bar, Journal of Chemical & Engineering Data, 59 (2014) 212-217.
[58] M.S. Shannon, J.M. Tedstone, S.P. Danielsen, M.S. Hindman, A.C. Irvin, J.E. Bara, Free volume as the basis of gas solubility and selectivity in imidazolium-based ionic liquids, Industrial & Engineering Chemistry Research, 51 (2012) 5565-5576.
[59] R. Fortunato, C.A. Afonso, M. Reis, J.G. Crespo, Supported liquid membranes using ionic liquids: study of stability and transport mechanisms, Journal of Membrane Science, 242 (2004) 197-209.
[60] P. Scovazzo, D. Havard, M. McShea, S. Mixon, D. Morgan, Long-term, continuous mixed-gas dry fed CO 2/CH 4 and CO2/N2 separation performance and selectivities for room temperature ionic liquid membranes, Journal of Membrane Science, 327 (2009) 41-48.
[61] S.U. Hong, D. Park, Y. Ko, I. Baek, Polymer-ionic liquid gels for enhanced gas transport, Chemical Communications, (2009) 7227-7229.
[62] B. Lam, M. Wei, L. Zhu, S. Luo, R. Guo, A. Morisato, P. Alexandridis, H. Lin, Cellulose triacetate doped with ionic liquids for membrane gas separation, Polymer, 89 (2016) 1-11.